AFRL-RH-WP-TR-2019-0071

Leaky Waveguide Full Parallax Holographic Video Display (LWFP-HVD) Phase I

Lloyd LaComb, Jr.,* Arkady Bablumyan,* Rick Rankin,* Armen Ordyan,* V. Michael Bove Jr, Sunny Jolly,** Bianca Datta,** Vik Parthiban,** Tyler Schoeppner,** Daniel Smalley,*** and Dylan Barton*****

*** TIPD, LLC, 1430 N 6th Avenue, Tucson AZ 85705-6644**
**** Massachusetts Institute of Technology, Cambridge MA 02139-4307**
***** Brigham Young University, Provo UT 84602-1231**

October 2019
FINAL REPORT

THIS IS A SMALL BUSINESS INNOVATION RESEARCH (SBIR) PHASE I REPORT.

AIR FORCE RESEARCH LABORATORY
711 HUMAN PERFORMANCE WING
AIRMAN SYSTEMS DIRECTORATE
WRIGHT-PATTERSON AIR FORCE BASE OH 45433
AIR FORCE MATERIEL COMMAND
UNITED STATES AIR FORCE

NOTICE AND SIGNATURE PAGE

Using Government drawings, specifications, or other data included in this document for any purpose other than Government procurement does not in any way obligate the U.S. Government. The fact that the Government formulated or supplied the drawings, specifications, or other data does not license the holder or any other person or corporation; or convey any rights or permission to manufacture, use, or sell any patented invention that may relate to them.

AFRL-RH-WP-TR-2019-0071 HAS BEEN REVIEWED AND IS APPROVED FOR PUBLICATION IN ACCORDANCE WITH ASSIGNED DISTRIBUTION STATEMENT.

HOPPER.DARREL.G.1231147264 Digitally signed by HOPPER.DARREL.G.1231147264 Date: 2019.12.03 16:46:30 -05'00'

DARREL G. HOPPER, Ph.D., DR-IV
Work Unit Manager, Sensory Interface Development Section
Airman Systems Directorate
711 Human Performance Wing
Air Force Research Laboratory

CARTER.LOUISE.ANN.1230249128 Digitally signed by CARTER.LOUISE.ANN.1230249128 Date: 2019.12.05 09:53:48 -05'00'

LOUISE A. CARTER, Ph.D., DR-IV
Chief, Warfighter Interface Division
Airman Systems Directorate
711 Human Performance Wing
Air Force Research Laboratory

This report is published in the interest of scientific and technical information exchange, and its publication does not constitute the Government's approval or disapproval of its ideas or findings.

REPORT DOCUMENTATION PAGE	Form Approved OMB No. 0704-0188

1. REPORT DATE *(DD-MM-YY)*	2. REPORT TYPE	3. DATES COVERED *(From - To)*
10-22-19	Final	31 Dec 2018 – 4 Oct 2019

4. TITLE AND SUBTITLE

Leaky Waveguide Full Parallax Holographic Video Display (LWFP-HVD) Phase I

5a. CONTRACT NUMBER
FA8650-19-P-6010

5b. GRANT NUMBER

5c. PROGRAM ELEMENT NUMBER
65502F

6. AUTHOR(S)

Lloyd LaComb, Jr.,* Arkady Bablumyan,* Rick Rankin,* Armen Ordyan,* V. Michael Bove Jr, Sunny Jolly,** Bianca Datta,** Vik Parthiban,** Tyler Schoeppner,** Daniel Smalley,*** and Dylan Barton*****

5d. PROJECT NUMBER
3005

5e. TASK NUMBER
V0

5f. WORK UNIT NUMBER
H0XJ (Historic: 3005V013)

7. PERFORMING ORGANIZATION NAME(S) AND ADDRESS(ES)
*TIPD, LLC, 1430 N 6th Avenue, Tucson AZ 85705-6644
**Massachusetts Institute of Technology, Cambridge MA 02139-4307
***Brigham Young University, Provo UT 84602-1231

8. PERFORMING ORGANIZATION REPORT NUMBER

9. SPONSORING/MONITORING AGENCY NAME(S) AND ADDRESS(ES)
Air Force Material Command
Air Force Research Laboratory
711 Human Performance Wing, Airman Systems Directorate
Warfighter Interface Division, Battlespace Visualization Branch
Wright-Patterson Air Force Base OH 45433

10. SPONSORING/MONITORING AGENCY ACRONYM(S)
USAF AFMC 711 HPW/RHCV

11. SPONSORING/MONITORING AGENCY REPORT NUMBER(S)
AFRL-RH-WP-TR-2019-0071

12. DISTRIBUTION/AVAILABILITY STATEMENT DISTRIBUTION STATEMENT A: Approved for public release; distribution unlimited.
Cleared 27 Nov 2019 by SAFPA, Case Number 88ABW-2019-5467.

13. SUPPLEMENTARY NOTES
This is a Small Business Innovative Research (SBIR) Phase I report developed under a purchase order for topic AF182-007 Field of Light Display for Air, Space, and Cyber Battle Management. Contains Patentable Information (patent being pursued but not approved).

14. ABSTRACT Final technical report for effort under topic AF182-007 describing the activities to develop an innovative holographic display system. To address the key DOD needs for future battlespace visualization, the current development team composed of TIPD, MIT and BYU modeled and developed key components of a prototype full parallax display based on leaky mode modulators. The system uses acousto-optic modulators to generate horizontal parallax and electro-optic phased array scanning to generate vertical parallax. The team developed several approaches for scaling the AO and EO modulator fabrication process compatible with volume production approaches. The team demonstrated a two-channel recirculating optical buffer integrated with the acousto optic modulator with a loss of 8dB. The optical buffer can be used to dramatically reduce the data transfer to the display. The report identifies direct laser writing and femtosecond laser writing as approaches that can be used to scale the system for volume production. An initial estimate of the bill of material and the size, weight, efficiency and power of the system are developed. The team developed a roadmap for future performance and efficiency improvements.

15. SUBJECT TERMS Field of Light Display, FOLD, Battlespace Visualization, Warfighter Interface, Air Space and Cyber Domains, Full parallax 3-D, Viewpoint Projections, Holography, Hogel, Direct Fringe Writing, LIDAR, SAR

16. SECURITY CLASSIFICATION OF:			17. LIMITATION OF ABSTRACT:	18. NUMBER OF PAGES	19a. NAME OF RESPONSIBLE PERSON (Monitor)
a. REPORT	b. ABSTRACT	c. THIS PAGE			Dr. Darrel G. Hopper
Unclassified	Unclassified	Unclassified	SAR	57	19b. TELEPHONE NUMBER *(Include Area Code)* (937) 255-8822

7Standard Form 298 (Rev. 8-98)
Prescribed by ANSI Std. Z39-18

TABLE OF CONTENTS

Section **Page**

LIST OF FIGURES

Figure **Page**

LIST OF TABLES

Table **Page**

FOREWORD

The PE65502F $149,999.00 SBIR Phase I purchase order FA8650-19-P-6010, Air Force Research Laboratory (AFRL) Workunit H0XJ Job Order Number (JON) (3005V013), was awarded to TIPD, LLC on 31 Dec 2018 with an end date 4 Oct 2019.

This effort was awarded under the SBIR Topic "AF182-007 Field of Light Display for Air, Space, and Cyber Battle Management" program. The OBJECTIVE and DESCRIPTION of this topic as published in Broad Agency Announcement (BAA) AF18.2 are provided below.

OBJECTIVE:
Develop and apply full-parallax solid-state digital Field of Light Display (FoLD) 3D visualization system written at video rates for interactive analysis of volumetric information from subsurface to geostationary earth orbit.

DESCRIPTION:
There are a broad range of applications of 3D displays to command and control problems, including Airspace Management & Deconfliction, Mission planning, Air Tasking Order (ATO) fly out, Combat Assessment, Integrated Air and Missile Defense (IAMD) Planning & Execution, Collection Planning & Management, Hostile sensor coverage analysis, Satellite orbit analysis, Chemical-Biological-Radiological-Nuclear and Explosive (CBRNE) incident plume analysis, surface mobility analysis, visualization of complex data states relative to geography, and space situational awareness. However, currently available true 3D displays have unacceptable levels of visual artifacts, do not provide full parallax, take too much power and space, require special headgear/eyewear, and preclude users from reaching into the image to control it. Visualization of inherently 3D situations—such as deconfliction, intervisibility, air operations, satellite constellations, terrain/building structures, and complex battlespace data—is significantly hampered when projected onto a 2D medium. The ultra-high information content of true 3D images relative to the 2D equivalents raises system bandwidth issues for the generation, storage, processing, transmission, and rendering of dynamic 3D visual data. The Field of Light Display (FoLD) class of 3D visualization system does not require the special eyewear nor have the accommodation-vergence conflict that characterize and limit applications of the Stereo 3D (S3D) class. Over the past 40 years several types (volumetric, integral ray, integral image) of the FoLD class have been fabricated, but technology barriers have inhibited implementations having acceptable space, weight, power, image quality, user interface, and cost. Recent research in processing power, algorithms, communications, wafer fabrication, and gesture control technology have now made it possible to develop a compact full multiplex FoLD class 3D battlespace visualization system. The technology developed in this topic must be scalable from individual/personal displays to multi-person/wall sized displays having power consumption, weight, and space footprint that can be accommodated in a command and control center environment. Metrics for image quality and metrology need to be defined and applied that are applicable to all types of FoLD system. A standard streaming model should be identified and implemented that are usable on all classes of 3D display. Interface should enable user control, annotation, and interaction with video and static imagery in real time. Prototype application focus for this topic is air, space, and cyberspace operations centers. No government furnished materials, equipment, data, or facilities will be provided.

1.0 SUMMARY

Analysts need improved three dimensional (3D) visualization tools to assist in critical situations such as deconfliction, line-of-sight analysis, air space and satellite control. Currently available 3D displays cannot provide the level of detail and comfort needed because the displays contain unacceptable visual artifacts, do not provide full parallax, require special headgear, and induce nausea in many of the users. The current visualization systems also do not have the capability to fuse static digital data with incoming LIDAR or video or allow the analyst to view the battle space from arbitrary points-of-view. To address the shortcomings of the current technologies, the proposal evaluated a novel display capable presenting a wide range of static and dynamic data. The system implemented a massively parallel computation and display engine capable of generating fringe information and directly "writing" the fringes using a novel display system employing acousto-optic modulators and electro-optic phased array scanning to generate the optical wavefront. This technique generates true holographic images and provides the operator with a full set of visual clues. This novel approach can be scaled to larger displays with higher angular resolution based upon the roadmaps of the underlying components.

The previous programs have demonstrated the technical feasibility of the key aspects of the target holographic video-rate display (HVD). The system is built around electro-optic and acousto-optics scanning subsystems fabricated with easy-to-scale lithographic techniques and a distributed GPU software algorithm capable of meeting the processing and integration targets of the program based upon published vendor roadmaps and algorithms improvements.

The ultimate goal of this research effort is to develop a full-parallax, solid-state 3D display with no mechanically moving parts. The target system should be capable of achieving video-rate display speeds with electronically generated holograms, require no special viewing apparatus, and be able to use streaming video and streaming geometry together with existing static content. The results of the base Phase II base program can be found in the Interim Report AFRL-RH-WP-TR-2016-0083.[1] The results of the Phase II extension program can be found in the Final Report AFRL-RH-WP-TR-2019-0008, 93 pp (Feb 2019).[2] The statement of work for the Phase I program is listed in Table 1.

Table 2 lists the key technical metrics required for an effective display. The LWFP-HVD Phase I program builds upon the previous research by TIPD, MIT and BYU during the HVD-GWSS Phase II[1] and Phase II Extension[2] efforts. The program incorporates previous research on holographic display system using acousto-optics scanning hardware architecture developed by MIT Media Lab[3] and the Visualization Management Software (VMS) developed under an IARPA SEEDLING holography program[4] awarded to TIPD. The Phase I program focused on further developing the acousto-optical scanning system, developing an optical buffer to reduce the data transfer requirements, and a roadmap to scale the display to a size (1m x 0.5m) suitable for use in Command and Control (CAC) environments, and develop metrics to assess the performance of the system. The Phase I program successfully demonstrated the capabilities of the optical buffer. The software effort was focused on demonstrating the technical feasibility of generating holographic data at rates supporting the minimum and objective configurations. The analysis indicated that data generation of 2 TB/s could be achieved with commercially available GPU hardware.

Table 1. Phase I Program Statement of Work

	Responsible
Task 1. Develop High-level System Architecture The contractor shall develop the system architecture for their LWFP-HVD approach to manage the holographic data from the generation software. The architecture will leverage existing OpenVMS software of the contractor which is capable of meeting the data generation requirements for the threshold FoLD system. The contractor shall use the display engine developed during the completed AF131-023 Holographic Video Display (HVD) Phase II Expansion program to generate the holographic data. The contractor shall identify any bottlenecks and develop possible solution**s.**	TIPD
Task 2. Integrate GV100 GPU and Measure Performance The contractor shall purchase, integrate, and measure the performance of a next-generation high performance NVIDIA Quadro GV100 graphical processing unit (GPU) or similar central processing unit (CPU). The contractor shall compare the results to forecasted improvement. The OpenVMS software will be optimized to determine the maximum possible calculation rate.	TIPD
Task 3. Design and Fabricate Prototype Circular Buffer (Fundamental Research) The contractor shall design and fabricate a circular buffer capable of recirculating the display signals. The circular buffer will be integrated with the existing leaky waveguide display prototype to evaluate its performance and compared to the model developed in task 4. The contractor shall optimize the performance of the device over the duration of the program.	BYU
Task 4. Develop and Optimize the Circular Buffer Model (Fundamental Research) The contractor shall develop a software model for the circular buffer and display system. The model will be used to predict and optimize the performance of the circular buffer. The model will also be used to estimate the signal degradation that may occur after N loops through the buffer. The contractor shall compare the results of the model to the experimental data collected from the device and incorporate the results into the next generation of the model and the device.	BYU
Task 5. Optimize Acousto-Optic (AO) Subsystem (Fundamental Research) The contractor shall optimize the existing prototype full parallax display from the HVD program using the optimized acoustic-optic modulator (AOM) subsystem with the electro-optic (EO) modulator to direct and project beamlets comprising the lightfield. The performance will be measured and compared to theoretical values.	MIT
Task 6. Integrate Subsystems into Display System The contractor shall integrate the subsystems developed in Tasks 2-5 and create an optimized LWFP display prototype. The contractor shall measure the performance of the prototype system.	TIPD

Table 1 Continued	**Responsible**
Task 7. Develop Next Generation Metrics for AO and EO Display The contractor shall identify measurement techniques and target values for critical system performance parameters using the existing standards as a baseline.	TIPD
Task 8. LWFP-HVD Design and SWEPPI Analysis The contractor shall design a complete FoLD system using their LWFP-HVD approach and the results of Tasks 1-7. The contractor shall analyze the SWEPPI parameters and issues this LWFP-HVD system design. The contractor shall prepare a preliminary plan for a Phase II effort.	TIPD
Task 9. Bill of Materials (BOM) Evaluation The contractor shall develop a BOM and ascertain assembly costs for prototype LWFP-HVD. The contractor shall determine cost and assembly feasibility for large area LWFP-HVD systems.	TIPD
Task 10. Develop Interaction Concept The contractor shall identify interactivity concepts to allow user interaction with the lightfield. The contractor shall evaluate these concepts and develop a design for one to be incorporated into a prototype demonstration unit.	TIPD
Task 11. Manage Program and Submit Reports The contractor shall perform program management, administrative and financial management functions during the course of the contract through reviews, teleconferences, reports, and meetings, as required.	TIPD
Task 12. Operational Security (OPSEC) The contractor shall provide OPSEC protection for all sensitive/critical information as defined by AFI 10-701 (Operations Security), the 711 HPW OPSEC Plan, and critical information list. The contractor shall participate in the 711 HPW sustained OPSEC awareness training or include OPSEC training as part of their on-going security program. The 711 HPW OPSEC coordinator will evaluate the OPSEC posture of AF contract activities and operations.	TIPD

Table 2. HVD-GWSS System Key Performance Parameters

Specifications	Threshold	Objectives
Parallax	Full	Full
Num. FP Display Elements	0.1MP	2MP
Full Conical Viewing FOV	45 degrees	90 degrees
Color	Monochrome	Full color
Update Rate	≥30 Hz	≥60 Hz
Pupil Spacing	4mm	4mm
Viewing Distance	36cm	36cm
Transfer rate in 2D Equivalent Pixels	490Mpixels/frame 15 Gpixels/sec	453Gpixels/frame 27 Tpixels/sec

Table 3 lists the key technical achievements of the LWFP-HVD Phase I program.
Figure 1(a) shows an oscilloscope trace of the signal before and after the recirculating buffer. The figure shows a 6dB loss.
Figure 1(b) shows an AO waveguide with a 26mm period printed using direct laser writing at MIT.

Table 3. Summary of Results for Phase I Program

Demonstrated an optical buffer with only 6dB loss
Demonstrated the capability to print the BYU AO modulator design using the direct write laser system at MIT
Developed direct writing techniques capable of printing phase and surface relief gratings
Designed, fabricated and tested 6.6ns switching arbiter circuitry to load new data or continue recirculating data in the optical buffer
Identified two separate GPUs capable of meeting the threshold display requirements
Demonstrated AO modulators capable of operating from 50 MHz to 70 MHz
Developed a roadmap for fabrication of a 1m × 1m display system
Developed preliminary BOM and completed SWEPPI Analysis

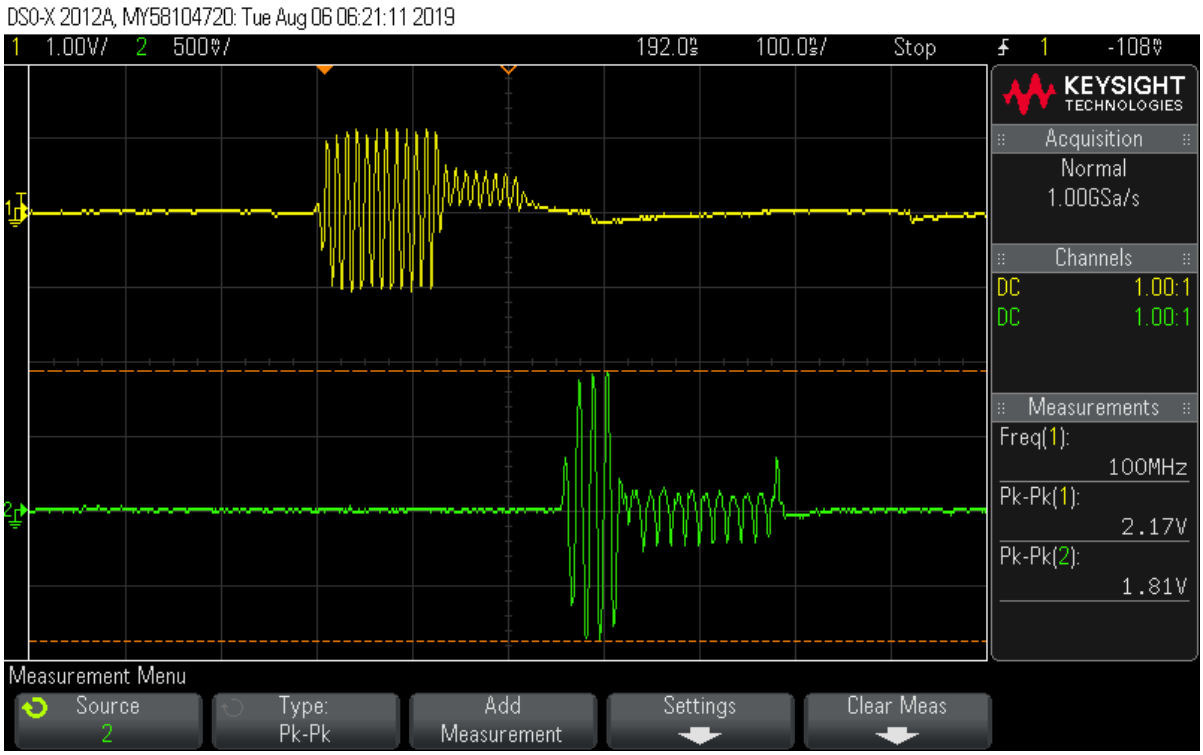

(a)

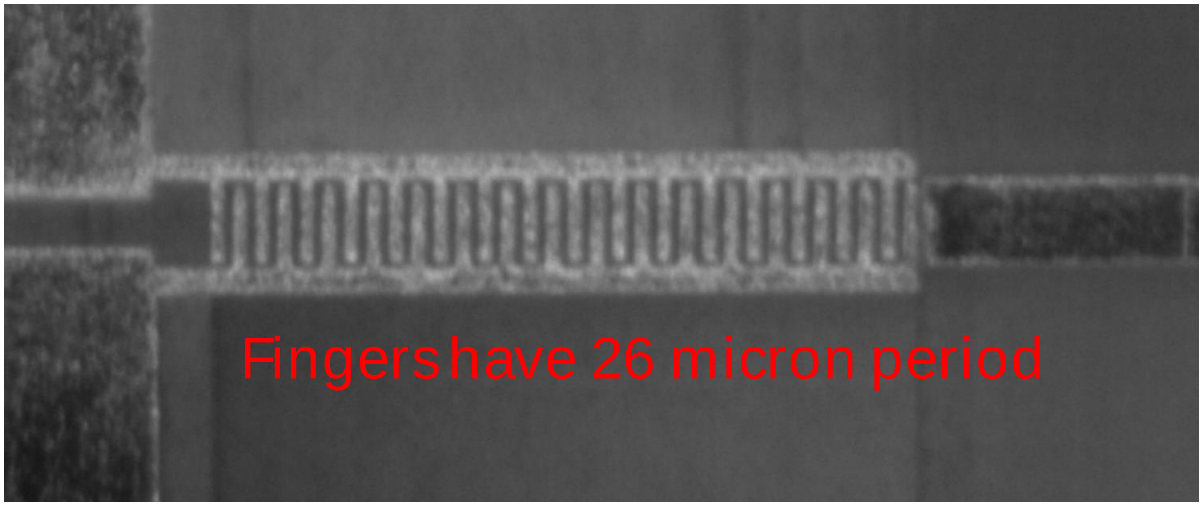

(b)

Figure 1. AO Modulator Development:
(a) Optical Buffer Showing Two-Channel Recirculating Signal;
(b) AO Modulator Produced by Direct Laser Writing

2.0 INTRODUCTION

Command and control battle maps and mission planning can be greatly enhanced by the representation of the battlefield in three dimensions (3D). Showing perspective views, depth and occlusions allows for a better understanding of the situation, and assists in avoiding errors when interpreting the terrain.[5] Digital Terrain Elevation Data (DTED) maps already exist and are in use, but are projected using two-dimensional display devices that limit their effectiveness. Streaming 3D geometric data from LIDAR and SAR is not currently available to operators, but is expected to become a critical component of battlefield planning within the next decade. As the Air Operations Center (AOC) modernizes its facilities, display systems capable of combining streaming data with existing DTED data will be required. The desire within the AOC for improved integration and visualization of existing and emerging visual data feeds is driving the need for a new approach to data display and management.

2.1 Background

Holography is a combination of two Greek words, *holos* meaning "whole", and *graphos* meaning "message". Optical holographs (or holograms) differ from photographs in that photographs record the intensity of the received light, whereas holographs record both the amplitude and the phase of the received light – thus providing the "whole image". By providing both the amplitude and phase information to the human visual system, the observer is able to perceive light as it would have been scattered by the real object without the need for any special eyewear. Capturing and projecting both the phase and amplitude of the optical signal separately for each eye allows the human visual system to perceive the object in three dimensions.

Holography was invented by Dennis Gabor in 1946 and rediscovered by Emmett Leith and Juris Upatnieks in the 1950's. Over the ensuing 65 years, a number of advancements have made holography accessible to various industries and holograms can now be found in artistic displays, on credit cards and as security devices on commercial software packaging. Various mathematical and optical techniques have been developed to simplify the hardware required to create holograms and to allow the holograms to be generated by a computer. A good overview of theory and practice of holography can be found in *Holographic Imaging* by Benton and Bove.[6] While various academic and commercial groups are actively involved in the development of holographic displays, none of these efforts has resulted in a full parallax 3D display capable of meeting the needs of the intelligence community.

Electronic holographic displays are based upon a spatial light modulator (SLM) which shapes or modulates the output light field based on the information flow from the computer containing the 3D data. SLMs have been constructed using various technologies including: liquid crystals (LC), micro-electrical-mechanical systems (MEMS)[7] and bulk acousto-optic modulators[8]. The current state-of-the-art modulators suffer from low bandwidth, small diffraction angles, the presence of large zero order signals, and quantization errors.[3] Recently, a new spatial light modulation technique has been developed using anisotropic leaky-mode acousto-optic modulation that offers a temporal bandwidth of up to 50 billion pixels per second (50Gpixel/sec).[3] The anisotropic leaky-mode modulator (ALMM) creates a surface acoustic wave (SAW) on the lithium niobate substrate with acts as the holographic diffraction pattern, which redirects the light. When the acoustic waves, which travel across the surface of the

anisotropic waveguide, are synchronized to the incoming light beam, the output signal is swept one direction creating the horizontal parallax display. Images generated by the ALMM are shown in Figure 2. Device measures 35 mm by 20 mm at the output of the display. Figure 2(a) shows a monochrome image and Figure 2 (b) shows an RGB modulation with continuous red, green and blue light (λ=633 nm, λ=532 nm, and λ=445 nm).[3]

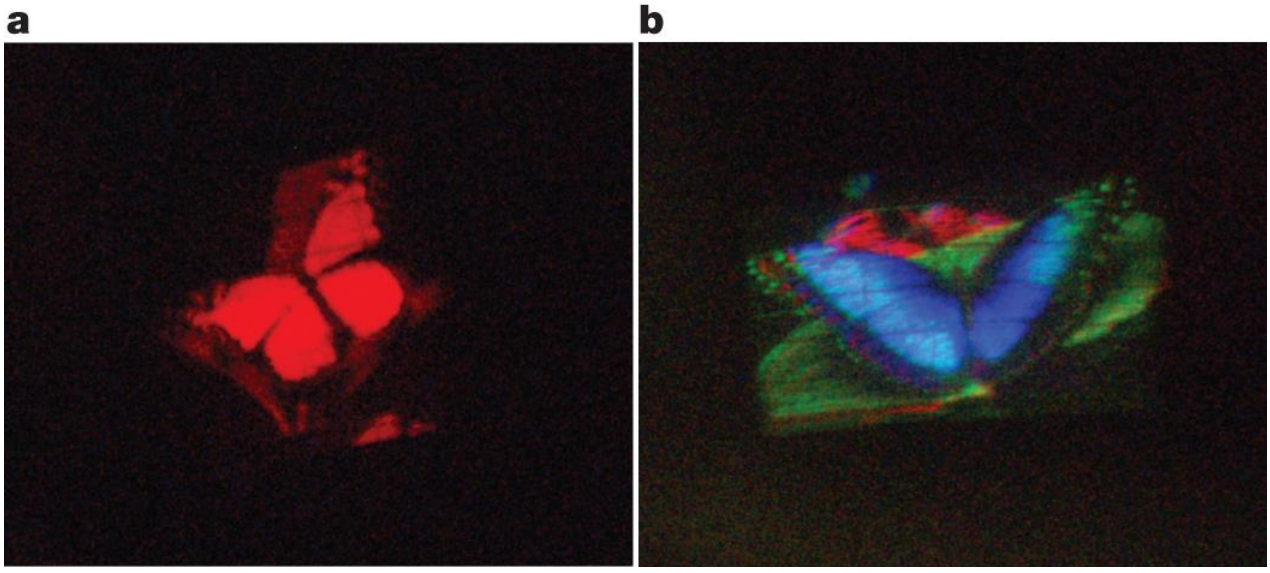

Figure 2. Single Channel Anisotropic Waveguide Holographic Stereograms

To create a full parallax display, the light field must be swept in the orthogonal direction to the ALMM. In the Phase I program, a lithium niobate electro-optic transducer was constructed to sweep the light field to create a full parallax display. In the HVD-GWSS program, the EO and acousto-optic modulators were integrated into a single device and test at a variety of wavelengths. A high level schematic of the combined two-axis scanning system is shown in Figure 3. To minimize confusion in this report, the acousto-optic scanning direction will be labeled horizontal direction and the electro-optic scanning direction will be labeled vertical direction. In Figure 3, light is coupled into the waveguide element via the input grating coupler. The light propagates and is separated into the sub-waveguides and the light in each sub-waveguide is retarded in phase by metal transducers (EO transducers) enabling vertical deflection of the output light. Additionally, a set of AO transducers produces a standing wave to diffract the light in the horizontal plane. The combination of these two gratings allows the waveguide element to focus output light to multiple points and steer it vertically and horizontally to form a holographic image.

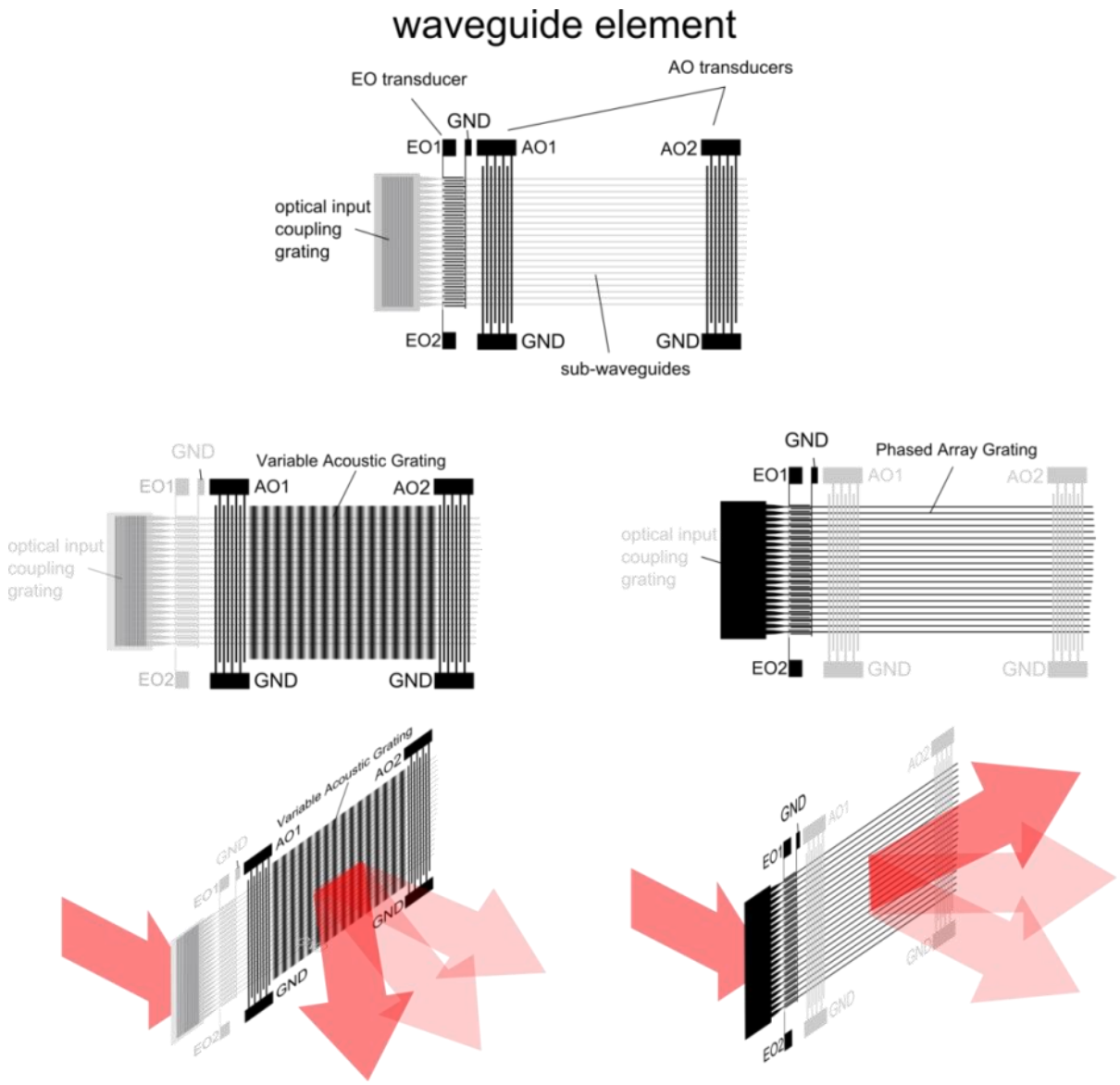

Figure 3. Two-Axis Non-Mechanical Scanning System

The second critical components of a video-rate holographic display for intelligence applications is the rendering algorithm. The rendering algorithm must be capable of generating all the data during one video frame cycle. The total number of bytes of data that must be generated and transferred per second (Ω) can be calculated using Equation 1.

$$\Omega\,(bytes/sec) = F_R \times N_H \times N_V \times N_\theta \times N_\Phi \times N_C \times N_B \qquad (1)$$

Where:

F_R is the number of frames per second to be displayed; 30 for the minimum target and 60 for the Objective configuration as described in Table 2.

N_H is the number of display elements in the horizontal direction

N_V is the number of display elements in the vertical direction and $N_H \times N_V$ is the Number of Display Elements listed in Table 2.

N_θ is the number of discrete views in the horizontal direction and θ is the horizontal component of the conical FOV as specified in Table 2.

N_Φ is the number of discrete views in the vertical direction and Φ is the vertical component of the conical FOV as specified in Table 2

N_C is the number of colors in the display (1 for monochrome and 3 for RGB)

N_B is the number of bytes per color channel (1 for this proposal).

The values of N_θ and N_Φ can be determined based upon the operator's viewing distance from the display and the properties of the human eye. The human pupil size varies based on the ambient lighting conditions - becoming larger in dark settings and smaller in bright environments. In a typical office setting, a pupil size of 4mm represents a good approximation to the "average" pupil size. To ensure smooth motion parallax, the display needs to provide new information at a minimum of every 4mm to match the pupil aperture. The viewing distance specified in Table 2 for a desktop display is 0.36m. Using these values, N_θ can be calculated using Equation 2.

$$N_\theta = \frac{2 \times 0.5\text{m} \times \tan\left(\theta/2\right)}{0.004\text{m}} \tag{2}$$

For the minimum configuration with $\theta = 45°$ horizontal cone angle, $N_\theta = 68 \approx 70$ and for the objective configuration with $\theta = 90°$ horizontal cone angle, $N_\theta = 275$. N_Φ can be calculated in a similar manner yielding values $N_\Phi = 70$ and $N_\Phi = 275$ for the threshold and objective configurations respectively. Our previous work has shown that in typical desktop viewing applications, the vertical cone angle can be one-third to one-half of the horizontal cone angle and still provide an acceptable viewing experience. For this report, we will assume the horizontal and vertical cone angles are equal. As the system progresses toward commercialization, the team will determine if the value of the vertical cone angle in the target application can be reduced. Inserting the values of the N_θ and N_Φ calculated from Equation 2 into Equation 1, the values of Ω for the threshold and objective configurations can be determined.

$$\Omega_{threshold} \approx 1.5 \times 10^{10}\ bytes/\text{sec} = 15\ GB/sec \tag{3}$$

$$\Omega_{objective} \approx 2.7 \times 10^{13}\ bytes/\text{sec} = 27\ TB/sec \tag{4}$$

Previous work by TIPD has demonstrated that multiple dedicated Graphical Processing Units (GPUs) can approach the rendering speeds needed for the LWFP-HVD program.

2.2 Synopsis of Work Performed During Previous Effort

In the HVD-GWSS Phase II program, the team demonstrated the key components necessary to implement a waveguided holographic display system based upon solid-state acousto-optic and electro-optic modulators that provide the scanning in the horizontal and vertical direction. During the base program, the team developed and refined the fabrication processes for creating the electro-optic and acousto-optic modulators and integrated them into a single device. The team developed a second-generation color encoding system capable of multiplexing the red, green, and blue signal channels into one signal that is swept horizontally and vertically by the AO and EO modulators. The modulators can be fabricated with significantly fewer lithography and processing steps than currently available SLMs providing a competitive cost advantage in addition to the improved angular performance and increased bandwidth.

The Phase II base program migrated the VMS software to Windows 7 and updated the libraries to be compatible with the currently released versions. A new computer and NVIDIA CPU combination was installed and the software has been migrated to the new platform. Initial testing has indicated a 7-fold improvement in full parallax performance with the new hardware and software. The team has developed an initial roadmap based on processes developed for the flat panel industry that could be capable of supporting a 1m × 1m full parallax holographic display suitable for intelligence and command and control applications. The team developed a geometric pyramid data model that is capable of asynchronous updates from streaming data. The data structure was updated with new image information and the time to update the data is within the tolerance for typical human interactions.

The key technical achievements of the HVD-GWSS program are in Table 4.

Table 4. HVD-GWSS Phase II Program Results Summary

Fabricated integrated electro-optic and acousto-optic modulators on the lithium niobate substrates
Demonstrated >15° deflection of the acousto-optic modulators
Demonstrated >5° deflection of the electro-optic modulators
Demonstrated at full parallax operation
Developed 2D and 3D metrics to evaluate the performance of the HVD system
Fabricated a 12-line display device with integrated acousto-optic modulators on the lithium niobate substrates.
Developed display software to drive multiple acousto-optic modulators with different frequencies and chirp single to determine the performance of the device
Demonstrated focusing of the acousto-optic modulators across ranges from 30cm to 3m.
Integrated signal outcoupling gratings with the acousto-optic modulators to demonstrate bottom surface imaging.
Demonstrated imaging with two simultaneous emitters.
Demonstrated of 28° horizontal beam scanning with acousto-optic modulators.
Demonstrated a software system capable of generating full parallax data across multiple GPUs producing holographic data at the rate of 0.48 TB/s and identified suitable GPUs to reach 2 TB/S.
Demonstrated AO modulator and grating fabrication using femtosecond laser processes.
Identified two potential vendors of low cost lithium niobate substrates.
Identified multiple techniques for lower cost production of AO and EO modulators
Developed a roadmap for fabrication of a 1m × 1m display system
Developed theoretical models to determine the point spread function as a function of focal distance and emitter position

3.0 METHODS, ASSUMPTIONS, AND PROCEDURES

The programmatic objective of the Phase I program was to demonstrate the viability of the technology. The MIT and BYU teams were responsible for demonstrating the AO and EO devices and the TIPD team was responsible for improving the rendering software and developing a roadmap to increase the size of the display.

3.1 Leaky Waveguide Fabrication

The procedure for fabricating the leaky waveguides is more fully described in Reference 1.

During the program, the BYU and MIT teams investigated simplifying the fabrication process by exploring techniques to direct write the grating using femtosecond lasers and to replace the time-consuming e-beam lithography step with a higher throughput laser writing process.

3.2 Lithography

In the HVD-GWSS program, the BYU team has transferred the writing process from the slow ESEM electron beam writer to the less expensive and faster Heidelberg µPG 101laser writer (https://www.himt.de/index.php/upg-101.html), Figure 4. In addition to the speed improvements, the team used the laser writer to develop a single process for printing full wafers with feature sizes down to 1µm. The AO and EO devices shown in this report were fabricated on the Heidelberg system.

Figure 4. Heidelberg Laser Writing System

3.3 Direct Femtosecond Laser Writing

In the previous Phase II program, the MIT team developed a femtosecond laser writing system with a computer-controlled stage for holding substrate material. The MIT team continued to investigate using the femto-second laser to replicate the gratings developed by the BYU team. During the Phase I program, the MIT team fabricated a waveguide with a 26μm period as shown in
Figure 1(b). The femto-second laser system can print lines as small as a few microns to generate waveguides capable of support higher frequency signals. The MIT team has scaled the femto-second laser system to be able to print larger structures including the bond pads for the acousto optical modulator.

Previous research has shown that due to the fundamental process involved in femtosecond laser pulse transmission through the media, it is only possible to alter the refractive index within a bulk material rather than on the surface. The refractive index variation within the material enables waveguides to be created by altering the refractive index between the core center and the cladding sides. The MIT team identified two different approaches for using femtosecond micromachining to create waveguides within bulk materials. The first approach uses MHz repetition rates, coupled with a low peak power laser pulse to produce isotropic refractive index changes in the bulk material. A second technique has been used to produce an anisotropic refractive index change to create birefringent refractive index material in the bulk material. This configuration uses a kHz repetition rate with high peak power.

Figure 5(a) shows the schematic design of the femtosecond laser system. Figure 5(b) shows the as-built system. The results obtained with the femtosecond laser writing system are presented later in the report.

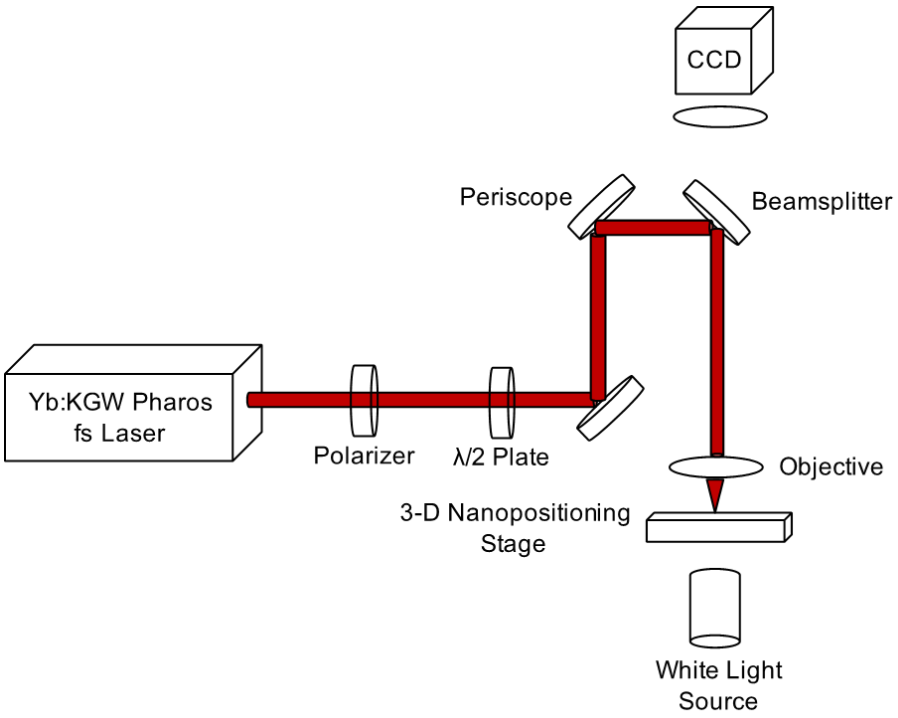

(a)

(b)

Figure 5. New Setup for Combined UV, Visible, and IR Femtolaser Micromachining

3.4 Computer Configuration for the Rendering Engine

The Tetrad-2 computer used in the Phase I program was scheduled to be upgraded to Windows 10 during the latter half of the program to test the latest generation of NVIDIA GPU cards. The upgrade to Windows 10 is required to support the latest generation of NVIDIA drivers. During the upgrade, there was a system failure and the computer has remained inoperable for the last two months of the program. The base specifications of the Tetrad-2 computer are shown in Table 5.

Table 5. Tetrad Hardware Specifications

Specification	**Tetrad-2**
CPU	2ea Xenon 2.5 GHz processors each with 10 cores
Ram	256GB
Bus to GPU	PCI-E 3.0 (x16) Bandwidth = 15.7GB/s
Graphics Card	4X NVIDIA Quadro K6000
GPU Memory/Card	12 GB
CUDA Cores/Card	2880
SPFLOPS	5196
DPFLOPS	1732
Memory Bandwidth	288 GB/s
Video Output	Max 4 outputs 2 Display Port 1.2 + DVI DL + DVI SL 4096x2160x60Hz + 2560x1600x60Hz + 1920x1200x60Hz

TIPD purchased two NVIDIA GPU cards during the program to evaluate the performance of the system.
Figure 6 presents a comparison of the relevant specifications of the two GPU cards.

SPECIFICATIONS

GPU Memory	8 GB GDDR6
Memory Interface	256-bit
Memory Bandwidth	Up to 416 GB/s
NVIDIA CUDA® Cores	2304
NVIDIA Tensor Cores	288
NVIDIA RT Cores	36
Single-Precision Performance	7.1 TFLOPS
Tensor Performance	57.0 TFLOPS
System Interface	PCI Express 3.0 x16
Power Consumption	Total board power: 160 W Total graphics power: 125 W
Thermal Solution	Active
Form Factor	4.4" H x 9.5" L, Single Slot
Max Simultaneous Displays	4x 3840x2160 @ 120 Hz 4x 5120x2880 @ 60 Hz 4x 7680x4320 @ 60 Hz
VR Ready	Yes
Graphics APIs	Shader Model 5.1[5], OpenGL 4.5[6], DirectX 12.0[5], Vulkan 1.0[6]
Compute APIs	CUDA, DirectCompute, OpenCL™

(a)

SPECIFICATIONS

GPU Memory	32 GB HBM2
Memory Interface	4096-bit
Memory Bandwidth	Up to 870 GB/s
ECC	Yes
NVIDIA CUDA Cores	5,120
NVIDIA Tensor Cores	640
Double-Precision Performance	7.4 TFLOPS
Single-Precision Performance	14.8 TFLOPS
Tensor Performance	118.5 TFLOPS
NVIDIA NVLink	Connects 2 Quadro GV100 GPUs[2]
NVIDIA NVLink bandwidth	200 GB/s
System Interface	PCI Express 3.0 x 16
Max Power Consumption	250 W
Thermal Solution	Active
Form Factor	4.4" H x 10.5" L, Dual Slot, Full Height
Display Connectors	4x DP 1.4
Max Simultaneous Displays	4 direct, DP 1.4
Display Resolution	4x 4096x2160 @ 120 Hz 4x 5120x2880 @ 60 Hz 2x 7680x4320 @ 60 Hz
VR Ready	Yes
Graphics APIs	Shader Model 5.1, OpenGL 4.5[7], DirectX 12.0[8], Vulkan 1.0[7]
Compute APIs	CUDA, DirectCompute, OpenCL™

(b)

Figure 6. NVIDIA GPU Specifications for Phase I Graphic Cards: (a) NVIDIA RTX 400 GPU; (b) NVIDIA GV-100 GPU

4.0 RESULTS AND DISCUSSION

The team made significant progress on the key technical objectives during the Phase I program. The sections below highlight the key technical areas of the program.

4.1 Acousto-Optic and Electro-Optic Waveguide Fabrication

The holographic video display is based on waveguide elements with variable AO and EO output gratings which offer significant advantages over other pixel-based methods of electroholography for full-parallax, full-color, video rate holographic display with a full complement of visual cues. The display is composed of an array of waveguide elements with a horizontal grating composed of standing acoustic waves and a vertical grating composed of an electro optic phased array as shown in Figure 7. Each waveguide element is subdivided into a group of sub-waveguides. A pair of cross-fired interdigitated transducers generates a standing surface acoustic wave. The resulting acoustic grating diffracts the light in the sub waveguides in the horizontal direction. Vertically, the sub waveguides form a phased array. Transducers on or straddling the sub-waveguides retard the phase of the light through the electro-optic effect. The phased array pattern, controlled by EO electrodes, allows arbitrary diffraction in the vertical direction.

The standard approach to electroholography involves diffracting light with a pattern of pixels which are in turn grouped into 'hogels'; the number of hogels defines the image resolution of the display while the number of pixels within a hogel determines the number of angular views that can be addressed. In the LWFP-HVD display, both the EO grating and the AO gratings are unconstrained in the horizontal direction so that a single waveguide element may be used to form one hogel or lengthened to form several hogels. In this context, a hogel becomes an element that is defined by the software rather than the hardware. In fact, for small displays (<5cm), a single waveguide element may be responsible for an entire horizontal line of the display. Figure 7(a) shows a small holographic display where one acoustic optic modular could be responsible for an entire line of the display. Additional lines would be added to increase the size. Figure 7(b) shows a holographic display of 1m x 1m or larger which could have a 1,000 × 1,000 array of waveguide elements which act as hogels. Pixel based holographic video displays with 60×60 views and 1000×1000 hogels would require a minimum of 3.6 billion connections because each diffractive pixel must be addressed directly. The LWFP-HVD system could be built with as few as five million connections for a large display and five thousand for a small display. A single pair of RF transducers controls hundreds or thousands of emitters, which can dramatically reduce the number of required connections.

The LWFP-HVD approach has a number of additional advantages over the current state of the art. The LWFP-HVD modulators can be batch fabricated on wafers using less than five mask steps (compared to 20 or more for active LC and MEMs devices). These devices are 'full color' and can simultaneously and independently modulate superimposed red, green and blue light using wavelength division multiplexing and therefore do not need any color filtering or temporal multiplexing of red, green and blue signals. Waveguide devices can be made to rotate the polarization of the output light with respect to undiffracted light, reducing noise. These devices produce no zero order and no conjugate image. These devices diffract light in an 'edge-lit' regime that provides as much as five times the angular deflection for a given pixel pitch when compared to devices illuminated by light normal to the display surface.

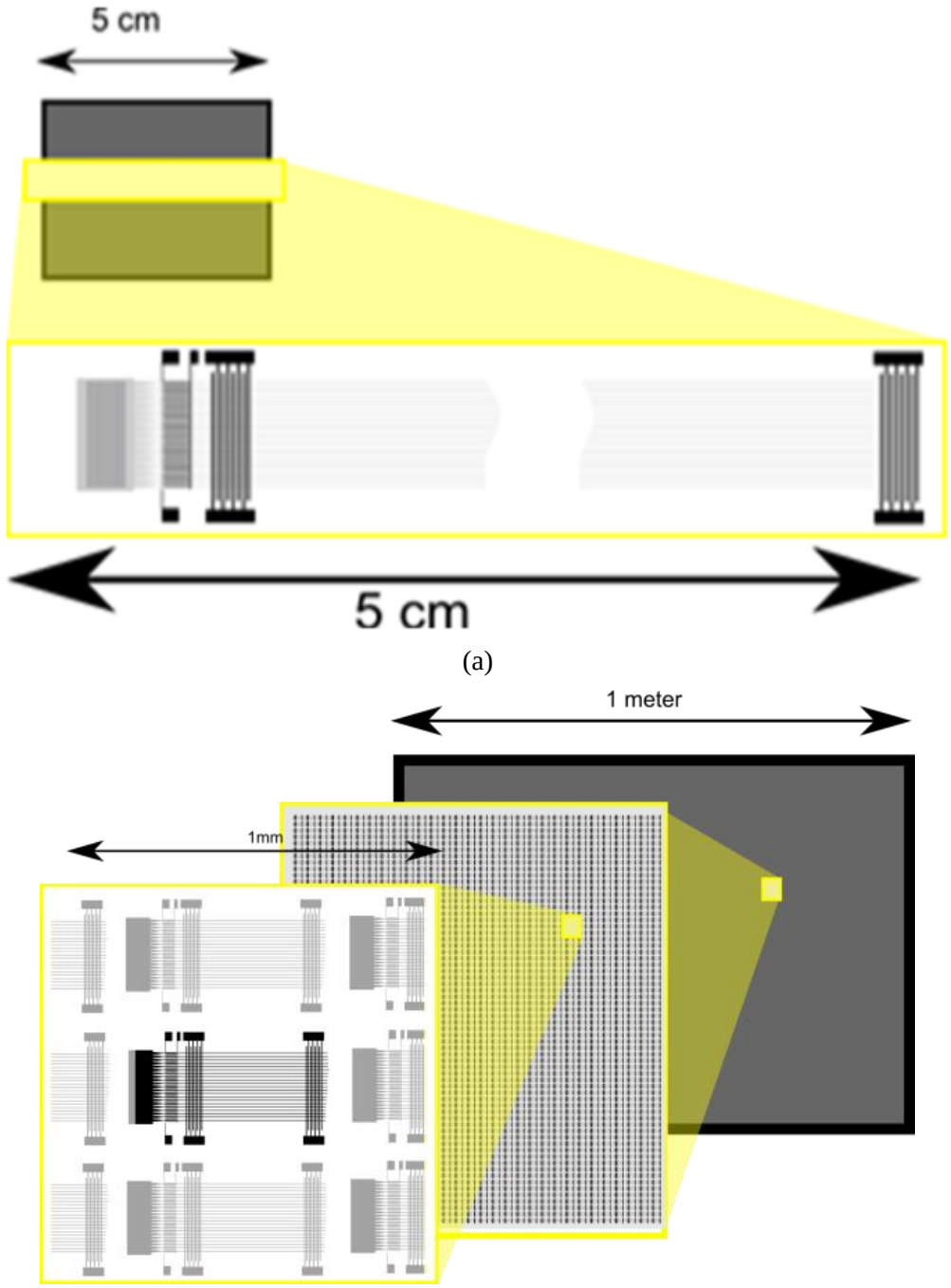

Figure 7. Full Parallax Display Concept

In the previous program, fabricated fully integrated AO-EO system as shown in Figure 8. Figure 8(a) shows a schematic of the device and Figure 8(b) shows a 100mm wafer with the integrated AO and EO devices.

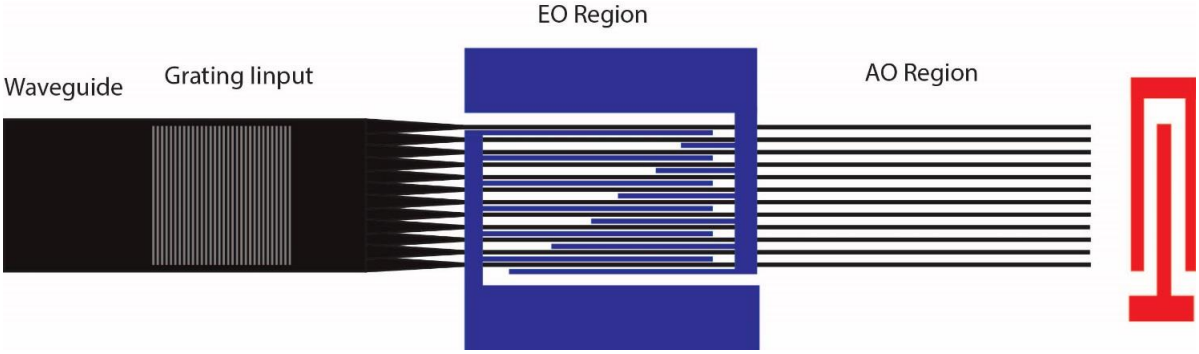

(a)

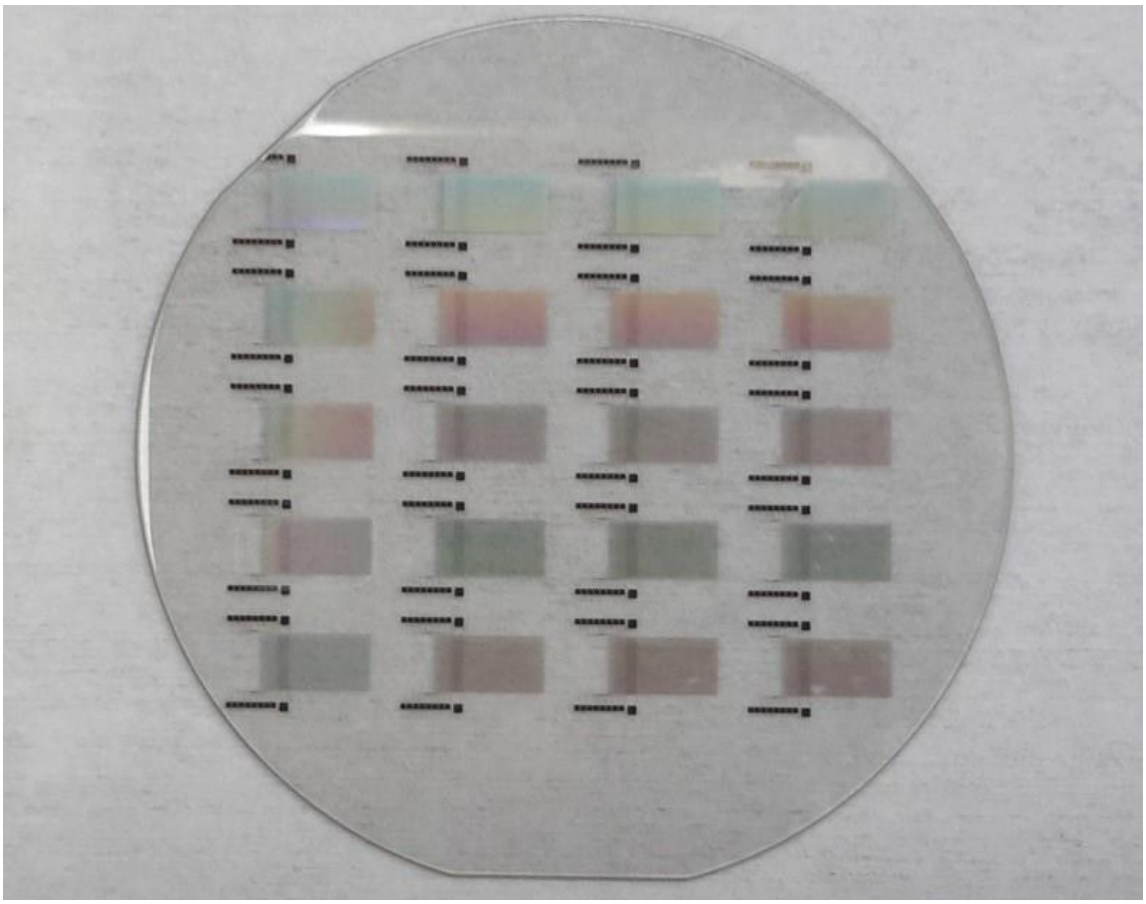

(b)

Figure 8. Integrated AO-EO Modulator System.

4.2 Circular Buffer

During Phase I, the BYU team focused on developing an optical buffer that would recirculate the signal applied to the AO modulator. In practice, most of the information in the field-of-light-display changes slowly relative to refresh rate of display. Implementing a recycling or recirculating optical buffer would reduce the amount of information that needs to be transferred from the computer to the display and minimize one of the bottlenecks in the system. The recirculating optical buffer receives the travelling acoustic wave at the end of the waveguide and converts it back to an electrical signal. The electrical signal is returned to the front end of the AO modulator where it is reinjected into the waveguide. To implement the recirculating buffer in the display, a fast electrics switch called the arbiter sits between the recirculating electrical signal and the input signal from the computer. If new information arrives from the computer, the arbiter passes the new information; otherwise the arbiter recirculates the signal. The acoustic to electric conversion is a lossy process and an electrical amplifier (not shown) is required to return the signal to its original strength. Figure 9 shows the schematic of the recirculating buffer.

Figure 10 is a picture of the completed recirculating buffer's electrical subsystem. The three SMA connectors bring the original source, recycled and arbiter signals to the arbiter (black IC at the center of the picture). The display signals are routed to the 12 waveguides at the bottom of the image. The BYU developed two generations of arbiters. The first generation had a switching time of 850ns, which proved to slow for the AO modulator signal. The second generation reduced the switching time to 6.1 ns providing a near step function response.

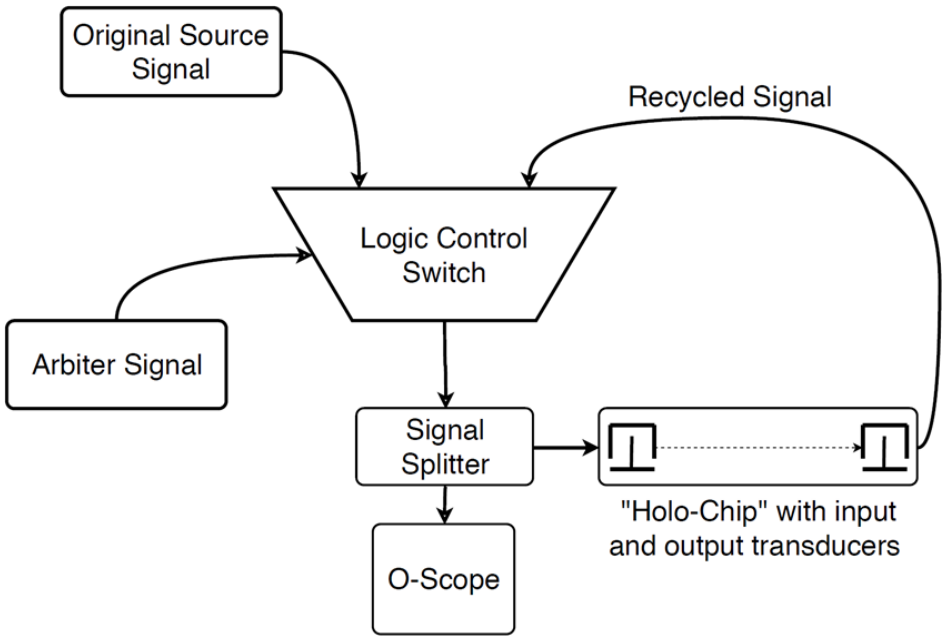

Figure 9. Optical Recirculating Schematic

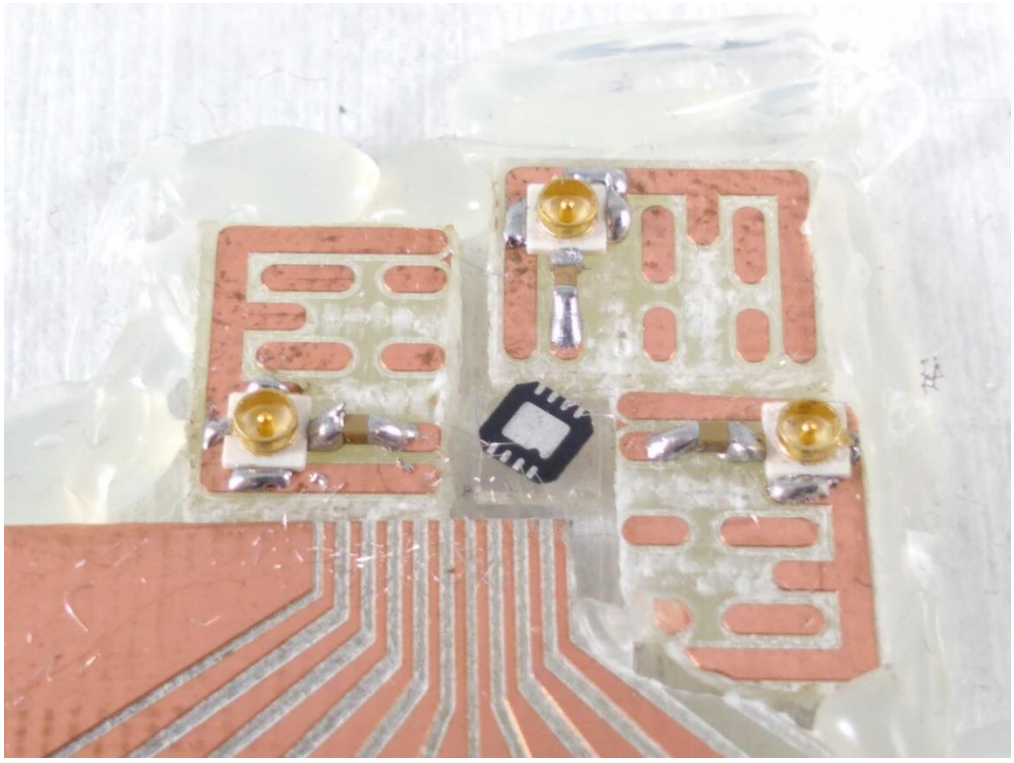

Figure 10. Recirculating Buffer Electrical Subsystem

In the first two months of the program, the BYU team designed the recirculating system and the final four months were devoted to optimizing the system to maximize the input efficiency and minimize the loss in the electrical system. The BYU team optimized the following factors to improve the performance of the optical buffer:

- Number of fingers
- Matching or mismatching number of fingers on input and output
- Distance between input and output
- Waveguide in center vs. empty
- Impedance match between the device and the incoming signal

Figure 11 shows examples of two sets of fabricated test devices. The left hand image shows a set of waveguides where the number of fingers was varied. The right hand image shows an experimental configuration where the distance between the input and output gratings was varied. For each transducer, the operating frequency and loss was measured (note the transducers were not impedance matched to the incoming signal). The team also explored the impact of having a different number of fingers in the transmission and collection structures and if having a region without any fingers improved performance. Losses varied from 70dB to 19dB. The best performing devices were electrically tuned to match the 50Ω impedance of the incoming signal. Figure 12 shows output from the network analyzer. The

recirculated signal is shown in Figure 11(a). The BYU team implemented a two channel multiplex system the oscilloscope traces of the two-channel system are shown in Figure 11(b). Both channels show recirculating losses of approximately 8dB.

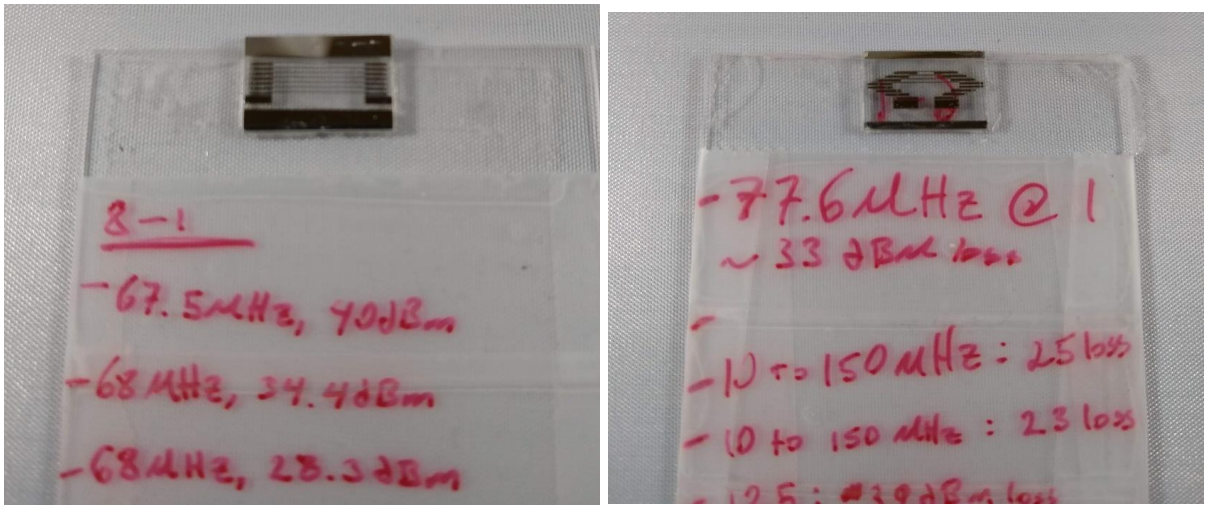

Figure 11. Transducer Designs: Testing Number of Fingers on Each Pair (Left); Various Distances between Waveguides (Right)

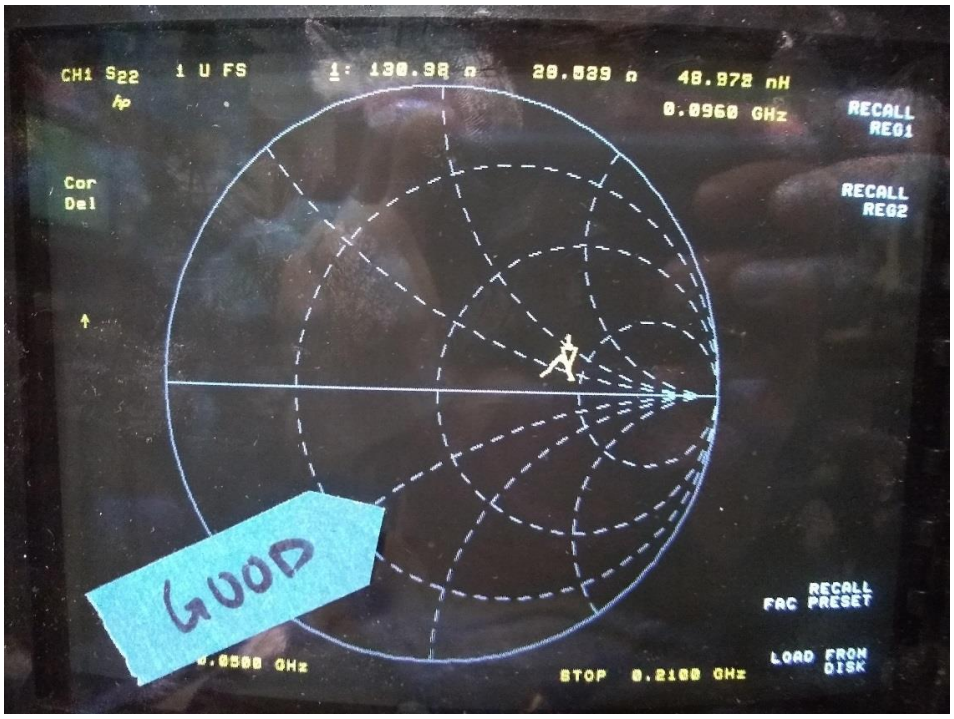

Figure 12. Post Fabrication Smith Chart

4.3 Optimize Acousto-Optic (AO) Subsystem

The MIT team investigated using the femto-second laser to replicate the gratings developed by the BYU team. The MIT team has developed a femtosecond laser setup with a computer-controlled stage for holding substrate material measured the characteristics of the printed waveguides. There are also known processes for creating conductive surface features using femtosecond lasers and if these can be used it would enable an entirely maskless, printed fabrication process. The experimental configuration is more fully described in Section 3.3.

The system is currently configured to produce and optimize a continuous isotropic refractive index change in Lithium Niobate. This target is achievable with a MHz high repetition rate and low peak power laser pulse. The MIT has built a Ti: Sapphire based femtosecond laser that operates at 85 MHz. The laser has a low peak power of approximately 400 mW and is tunable. This base laser system is tunable through an additional Pockels cell system that allows for the reduction of power to 0 mW offering the micromachining control of tuning the light intensity from 0 mW to 400 mW.

Five primary parameters affect the resolution and thus the accuracy of the point ionization. These parameters are the spot size due to the numerical aperture (NA) of the objective lens, the light intensity, the exposure time, the wavelength of the femtosecond pulses, and material selection. The team has developed a system that controls all five of these primary parameters. The light intensity is controllable through the Pockels cell. The NA of the system is controlled through the objective lens. Currently, the system uses a high numerical aperture achromatic lens as our objective lens with a 20 mm focal length and a 20 mm diameter offering an NA of 1. It is preferable to apply high NA lenses with the lower power as they offer a shorter depth of field and enable one to focus on a smaller spot.

The system is designed so that the amount of energy imparted to the material can be controlled indirectly through two mechanisms. One mechanism to controlling the exposure energy is to control the velocity of the stage and to control the amount of time a material is exposed. The second mechanism is to control the intensity of the beam through the Pockels cell. The Pockels cell controls the intensity from a range below ablation to a point below ionization. Within this intensity range, the materials refractive index is altered through densification of the lithium niobate. This dynamic range enables us to determine various amounts of photoionization and determine the effects that these low intensities have on our resolution spot. This double mechanism approach enables both mechanical and charge based mechanisms to control the exposure time. Exposure time is controlled for each location by tuning the intensity with the Pockels cell rather than scanning across the surface. The Pockels cell tunes the intensity through a voltage input between an artificial "off" position, which is below the ionization energy of a material to a position where structural densification can occur to induce a change in refractive index.

In the Phase I program, the MIT team fabricated a waveguide with a 26μm period as shown in Figure 1(b). The femto-second laser system previously demonstrated the capability to print lines as small as a few microns.[2] The MIT team has scaled the femto-second laser system to be able to print larger structures including the bond pads for the acousto optical modulator. Figure 13 shows the entire acousto optical system fabricated using the fs laser.

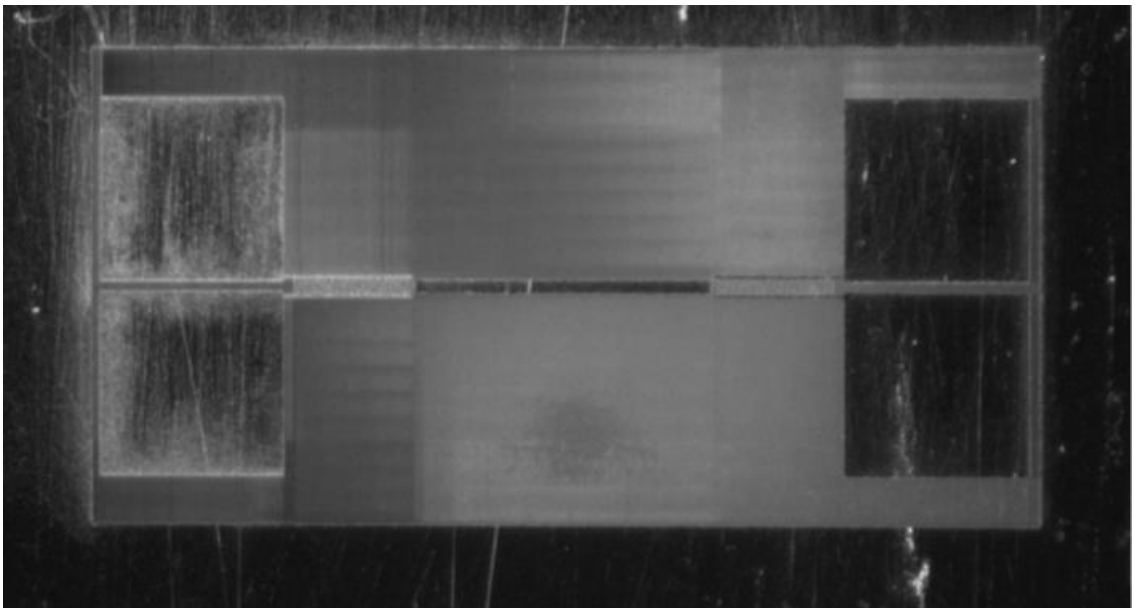

Figure 13. Waveguide and Bond Pads Printed Using Femtosecond Laser

The MIT team investigated phase grating as an improved outcoupling mechanism. The best performing gratings will be used in the next generation system. The MIT team also explored different approaches for optimizing grating patterns as shown in Figure 14. The new approach involves starting with the grating seen in nature, evaluating the reflectance and then changing the structure and repeating the process until a local optimum is achieved. The initial experiments produced outcoupling grating that could be manufactured using high volume fabrication methods as shown in the scanning electron microscope (SEM) micrograph in Figure 15.

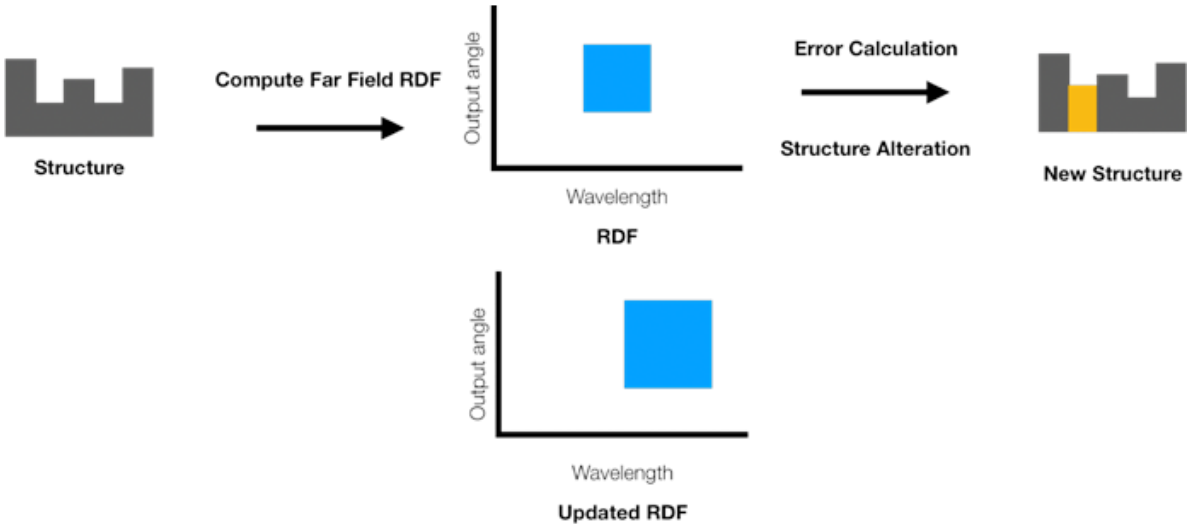

Figure 14. Grating Optimization

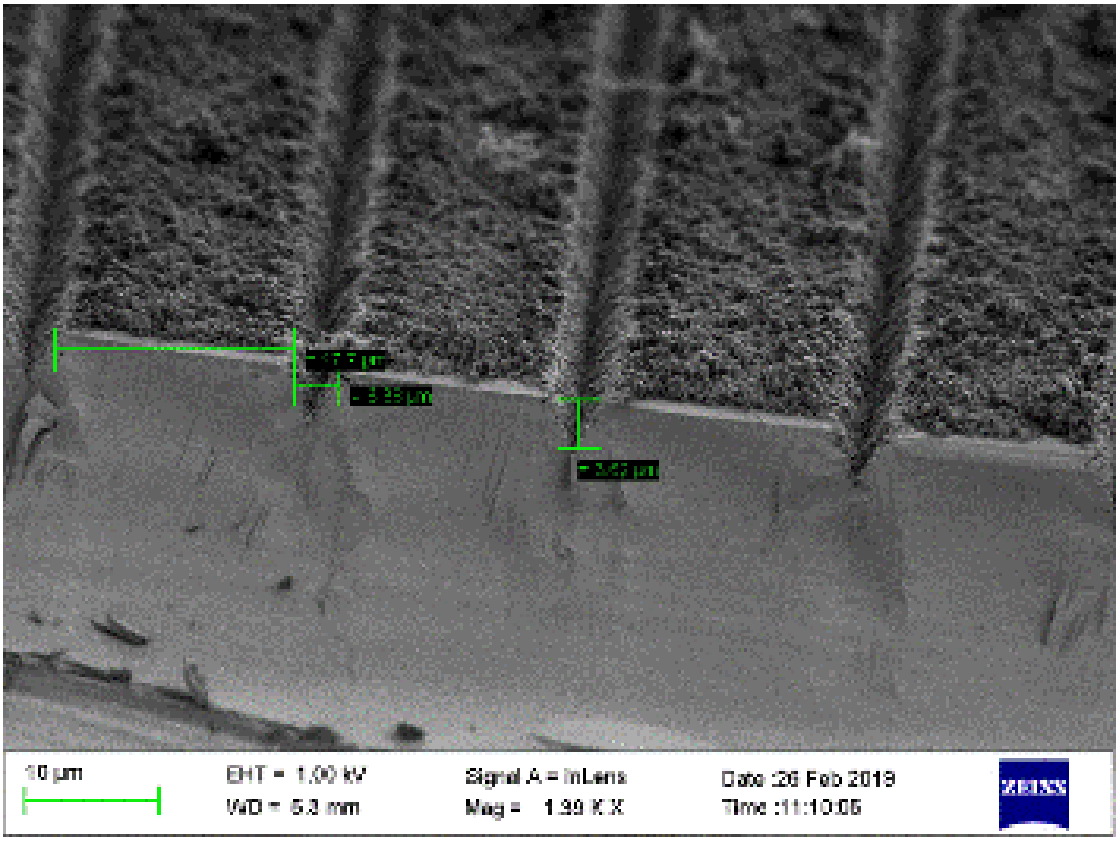

Figure 15. SEM Micrograph of Output Phase Grating

4.4 Rendering Engine

The second key challenge in developing a video-rate holographic display is creating, managing, and transporting the terabytes of information to the HVD. As outlined in equations 3 and 4, the rendering engine requires continuous data generation at rates between 15 gigapixels/s and 27 terapixels/s. This level of data generation far exceeds the capabilities of a single PC-class computer and is similar to the processing provided by special-purpose super computers. Rather than develop a custom-built and expensive computer system, the team investigated building the rendering engine around commercial-off-the-shelf (COTS) components. Using COTS components offers several advantages including shorter development time, lower component costs, and the ability to leverage performance improvements that are driven by the larger PC, tablet, and mobile consumer marketplaces.

In the previous program, the team evaluated approaches based on two commercially available alternatives. The “big iron” approach used a small number of high-powered GPU to perform the calculations and the “small iron” approach used a large number of small “lightweight” system-on-a-chip processors that are used in cell phone and tablets. Both approaches were evaluated based on data collected from prototype systems, published industry roadmaps and discussions

with NVIDA, AMD and Intel. The "big iron" approach was selected and all work in the Phase II expansion program was performed on the Tetrad-2 system.

The challenge of displaying a full color hologram can be addressed by multiplexing the RGB signals onto one signal that can be coupled to the display. With appropriate fabrication parameters, anisotropic leaky-mode modulators can be made to allow for the simultaneous and superimposed modulation of red, green, and blue light in a wavelength-division multiplexed fashion. A more thorough mathematical analysis of the RF signals is provided in the HVD-GWSS Phase I Final Report.[9]

The initial target system is designed to support a 100,000-element display with 3-color hogels where each hogel supports a conical FOV of 45° updating at 30 Hz requiring a system architecture that can handle a sustained data creation and display rate of approximately 45 GB/s. The current program builds upon the Visualization Management System (VMS) developed in the IARPA SEEDLING program (FA8650-10-C-7034) and extended under the Phase II HVD-GWSS program (FA8650-14-C-6571). The Phase II program demonstrated a system capable of generating data at a rate of 0.48 TB/s or approximately ten times the minimum configuration data rate.[1]

In the Phase I program, TIPD evaluated two possible GPU configurations. The specifications for the two GPUs are shown in
Figure 6. The initial plan was to purchase the NVIDIA Quadro GV100 system and evaluate its performance. The GV100 is one NVIDIA's most powerful GPU systems and is optimized for scientific, financial, and engineering applications. In November 2018, NVIDIA announced the Quadro RTX 400 system based upon their Turing Architecture.[10] The GTX 400 has several advantages over the GV100 system including higher video output bandwidth, smaller form factor and significantly lower cost while it has less on board memory, fewer CUDA cores, and approximately one-half the floating point performance. The current Tetrad computer system can hold four GV100 or eight RTX 400 cards that would provide roughly equivalent floating-point performance. The eight RTX 400 cards could provide 32-8K video outputs capable of >60 Gpixels/second compared to 15 Gpixels/second for a four GV100 system. The other significant advantage of the RTX 400 is the eight RTX cards would cost approximately $8K, while four GV100 cards would cost over $40K. TIPD ordered and received both the RTX400 and GV-100 systems. The new cards are only compatible with Windows 10, which required an operating system upgrade to the Tetrad-2 computer. TIPD attempted to upgrade the computer to Windows 10 in order to work with the next cards but the upgrade encountered problems and has been delayed while the vendor rectifies the problem.

Additional performance improvements can be achieved through architectural and algorithmic changes. The current algorithms have not been optimized for vertical parallax data generation and some of the techniques used in making the horizontal parallax insensitive to number of views may be applicable to the vertical parallax calculations. The team has also investigated changing the order of the calculations to make the algorithm insensitive to the number of horizontal display elements rather than being insensitive to the number of horizontal views in the current algorithm. This change could potentially offer a 5X-10X improvement in the frame rate. The initial analysis looks promising, but any changes in the data flow will need to be evaluated

based upon the format of the data to optimize the display time. The current algorithms also allow the OpenSceneGraph (OSG) code to determine the size of the data cache kept in the CPU's RAM and the size of the data pyramid. These parameters can be optimized once the typical use cases are identified during the software requirement phase. If the data sets are small, it may be possible in the Tesla series graphic cards to download the entire pyramid into graphics memory thereby eliminating several steps in the process. This approach would not scale to large data sets but might be an option based upon the end-user use case scenarios. Figure 16(a) shows the display and Figure 16(b) the processing performance of the previous GPU and a fully configured computer with 4-GV-100s or 8 RTX-400 GPU. Note the log scale in both plots.

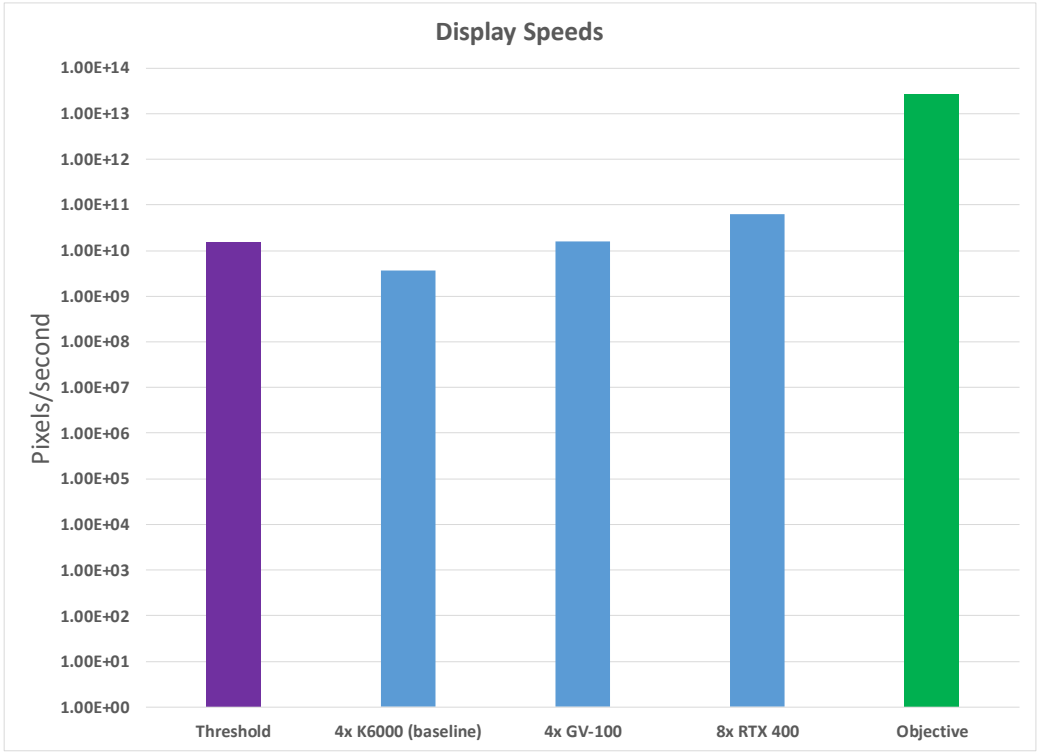

(a)

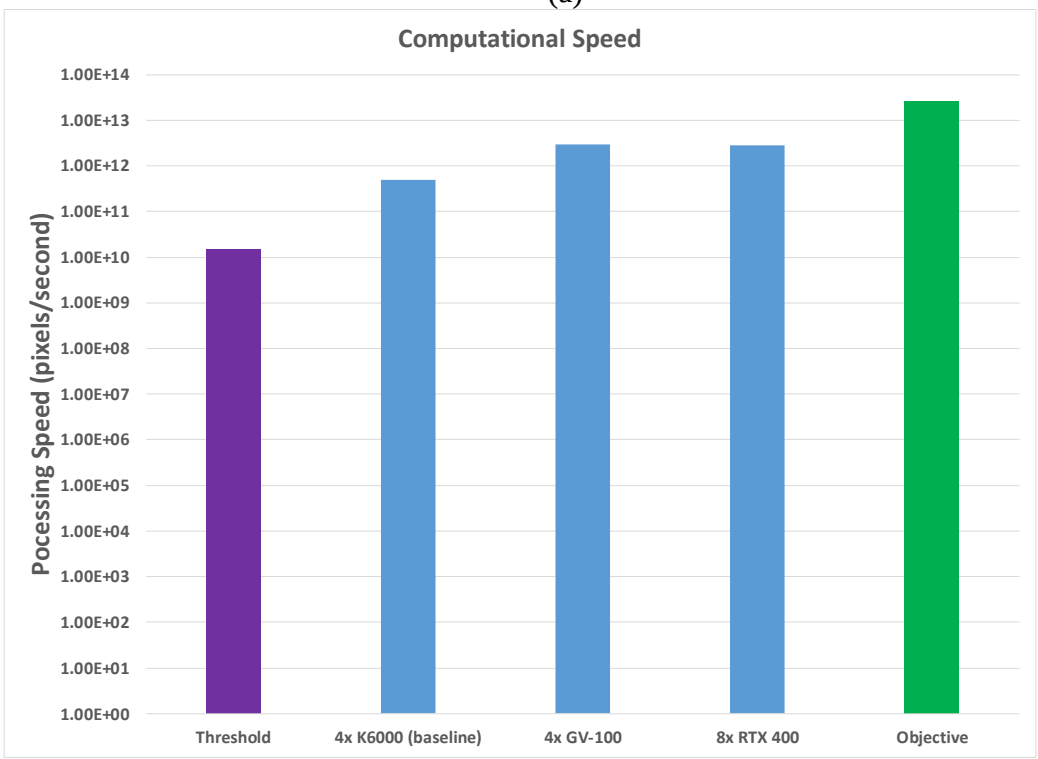

(b)

Figure 16. Display and Computation Comparison: (a) Display Speed; (b) Computational Speed

4.5 Roadmap and Commercialization

The team investigated a number of processes and technologies that could dramatically reduce both the cost and time to fabricate the holographic display. Two key items that would need to be addressed to accelerate the adoption are expanding the display size and simplifying and automating the manufacturing process to improve the repeatability and reduce the cost.

Expanding the size of the display requires leveraging existing mass production technologies used by the flat panel display industry. After a thorough search of available materials and processes, the team determined that lithium niobate is the only commercially available material that has required mechanical (piezoelectric and sound velocity) and optical properties (transparency across the visible) for the LWFP-HVD applications. DOD and academic researchers have been investigating alternatives to the traditional methods of fabricating crystalline lithium niobate without success. These two outcomes motivated the team to look for approaches to fabricate a large panel from smaller crystalline lithium niobate substrates without introducing artifacts into the display. This approach, shown in Figure 17, affixes rectangular lithium niobate substrates to a large glass panel. The figure shows how a 600mm display could be assembled from 70mm x 70mm LiNbO3 square substrates. The assembled glass-lithium niobate subassembly can then be lithographically printed in one operation using the processes described above to create the display. This approach ensures that lithography does not introduce any artifacts into the display. The large lithium niobate sheet could be printed using the femto second laser system, the Heidelberg printer or any system capable of printing on large sheets.

The modular approach allows the team working on improving the individual hogel display module to proceed independently from the team working to integrate the hogel display modules into the larger display. This approach also allows improvements in the performance of the hogel display modules to be incorporated into the display as soon as they become available.

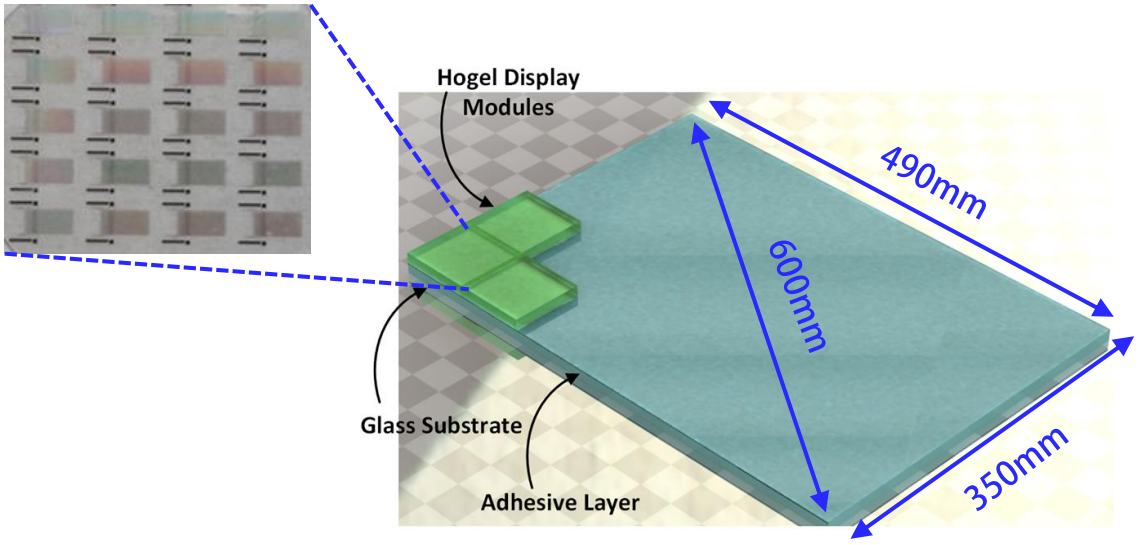

Figure 17. Large Display Schematic

Samsung has adopted a similar modular approach for their new microLED televisions branded as "The Wall".[11] The system uses approximately 300mm x 300mm panels each composed of smaller subsystems that can be connect to form a larger display. The process provides both electrical connection and minimal artifacts even at high viewing angles. While a FOLD display with its angular specific information may show artifacts not visible with an omnidirectional television display, the basic concepts have been developed to at least a prototype production level.

The modular approach may also simplify the interaction between computation and the display subsystems. In one approach, the computation and display engine throughput could be matched as shown in Figure 18. Figure 18(a) shows the single computation engine and display and Figure 18(b) shows a tiled system integrated to make a larger display. This approach could have several advantages over a monolithic approach including allowing the team to pursue the independent development of the electronics and display, and simplifying the development and fabrication processes.

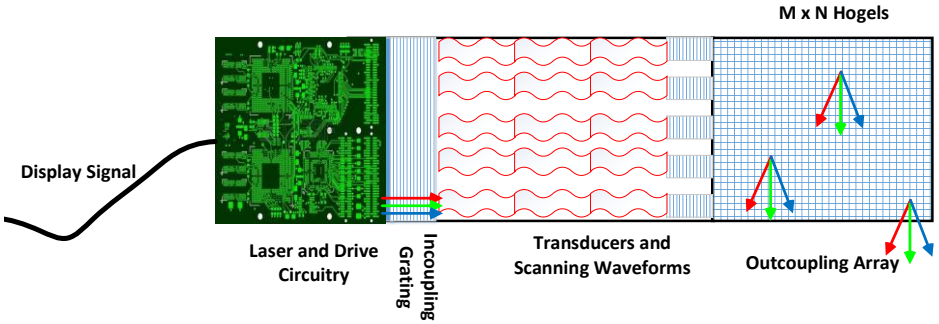

(a)

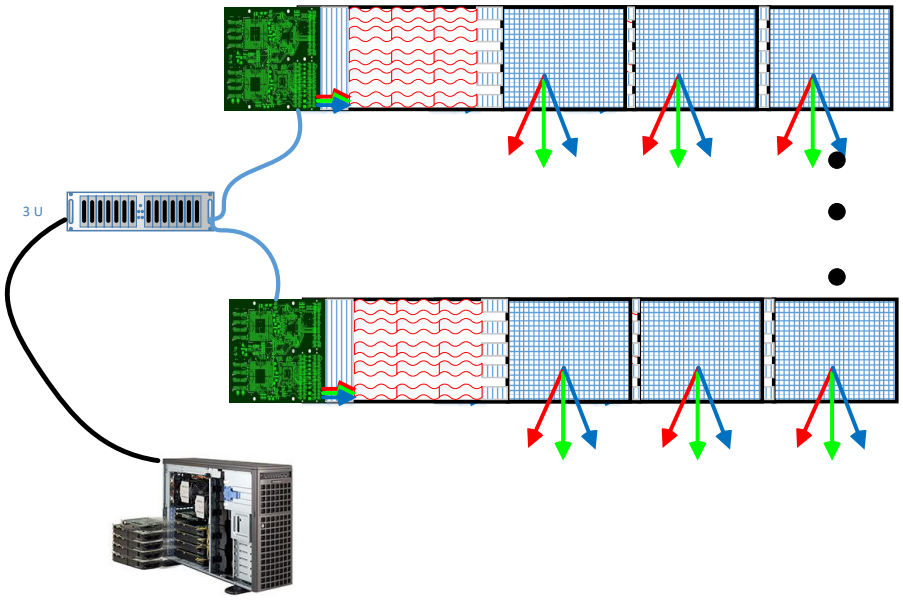

(b)

Figure 18. Integrated Subsystems Conceptual Schematic:
(a) Single Computational Engine and Display; (b) Tiled System Large Display

The team studied two of the potential artifacts to determine their potential impact on the display. The first artifact that was studied was the potential impact that the edges of the lithium niobate wafers may have on the display. Fortuitously, one of the test devices cracked during testing. The sample was polished to clean the edges and reinserted into the display system. The display system performed as expected indicating that it should be possible to minimize or potentially eliminate the visual impact of the tiled lithium niobate substrates.

TIPD identified four possible approaches to create $LiNbO_3$ material for use in a large display. The first approach would be to work with our existing lithium niobate supplier, Gooch and Housego, to produce rectangular substrates with optically flat edges that would be placed in optical contact with each other. Our previous work has shown that highly polished substrates can be placed in contact with each other and the diffracted light can traverse the interface without introducing visually noticeable artifacts. The other three approaches involve affixing the lithium niobate directly to the substrate glass.

NANOLN (Peoples Republic of China) uses a proprietary process to fuse lithium niobate to insulating materials. The process is capable of replacing the lithium niobate substrate and SiO_2 layers s with a glass substrate. NANOLN is capable of providing up to 900nm of X-cut single crystal lithium niobate using this technique.

Partow Technologies (Vista, CA) has developed two methods for creating a lithium niobate film on a glass substrate. The first method uses an ion beam to prepare the lithium niobate for bonding to the glass substrate. The treated lithium niobate is fused with the glass substrate under heat and pressure and the top layer of the lithium niobate is removed using ion slicing. The top surface is polished to the desired flatness and the remaining lithium niobate substrate can be recycled and used in the next bonding operation. This technique can be used to produce lithium niobate thicknesses up to 900nm.

The second technique bonds the lithium niobate wafer to the glass substrate and then polishes the substrate to the desired thickness. This method is capable of producing lithium niobate thickness of up to 5 microns. TIPD is working with both companies to understand the processes and performance characteristics. Both techniques look promising for scaling the device side beyond what can be fabricated on a single lithium niobate wafer.

4.6 BOM and SWEPPI Analysis

During the Phase 1 program, the TIPD completed a preliminary BOM (Bill of Materials) and SWEPPI (Space, Weight, Ergonomics, Power, Performance and Integration) analysis of the proposed system. In the analysis, TIPD used the actual prices paid for material and estimated the potential pricing discount that could be achieved if the system went into volume production. The size, weight and power of the display is based on an engineering estimate based on the scaling of the small display prototypes.

TIPD completed an initial market survey and identified several key performance indicators.

- System electrical power: Powered by 1 (minimum) or 2 (maximum) 15A 115V A/C. 1.5 – 3KW
- Size: Integrated into workstation – Size of two desktop computers + display that fits on desktop and allows analysist access to keyboard and interactive device
- Weight: Moveable by two warfighters. Entire system: less than 125 lbs.

Table 6. SWEPPI and BOM Summary

	Size	Weight (lbs.)	Power (W)	Cost at unit 10	Cost at Volume	Comments
Computer	18" x 7" x 26"	85	Maximum: 1620	$ 1,457	$ 1,200	Weight Includes cards Power is maximum supported power including GPU cards Weight includes redundant power supplies
GPU Cards						
Option 1: GV-100 (4)	in computer	in computer	1000W included in computer max	$36,796	$32,000	
Option 2: RTX400 (8)	in computer	in computer	1280W included in computer max	$7,120	$ 6,000	
Display	49 cm x 35 cm 20" x 14" Depth: 12"/ 30cm	50	TBD			
Lithium Niobate Substrates	included in above			$22,500	$15,000	Estimate based on 100mm wafers
Glass Substrate	included in above			$250	$100	
Electronics and Light sources	included in above		TBD	$28,000	$17,500	Price could be less depending on level of electronics and photonics integration
Assembly and Testing				$20,000	$5,000	
Estimated Total		135	TBD	$109,003	$70,800	

Table 6 lists TIPD's estimated BOM and SWEPPI values.

Table 7. Performance Metrics for LWFP-HVD

Parameter	Value
2D Metrics	
Number of display elements	1M for minimum system; 2M for objective system
Contrast	> 10:1, target > 50:1
Brightness	> 50 cd/m^2; target > 100 cd/m^2 within FoV cone
Color Alignment	90% of display elements < 1/5 element; < ½ display element max
3D Metrics	
Horizontal Viewing Cone	Minimum 30°; target 60°
Vertical Viewing Cone	Minimum 30°; target 60°
Contrast, brightness vs angle	Minimum total indicated range < 10%
Modulation Transfer Function vs projection distance and angle	TBD
Accommodation-vergence mismatch vs. observer position	TBD; target << 10% of viewing distance
Hogel Generation	
Frame rate	30 fps full parallax for minimum system; 60 fps full parallax for objective system
Time to 3D image update after new data tiles received	Target 0.25 seconds

4.7 Metrics

The Phase I program has identified a number of key metrics that can be used to validate the imaging performance of the system during later development programs. The key metrics are listed in Table 7.

The team attended several conferences to discuss metrics and standardization during the previous Phase II program. The conferences had lively discussions on standards and metrics. The conferences were organized by Third Dimension Technologies and Insight Media and funded through AFRL SBIR program. The team held discussions with various parties including the JPEG PLENO team, the SMPTE COMPCINE working group, and the MPEG standards groups. There was no consensus on key metrics or overarching standards which might be employed in FOLD systems or if certain metrics would be more useful in some applications. In many cases, there did not seem to be a clear approach on what criteria should be considered when comparing the different approaches.

The team met with the FOVi3D team to review their testing protocol. The team agreed to exchange details of the display system and evaluate if the FOVi3D system could be used to test the LWFP-HVD system when it reached the prototype stage.

5.0 CONCLUSIONS

The LWFP-HVD Phase I program demonstrated the key components necessary to implement a waveguided holographic display system. The system is based on electro-optic and acousto-optics scanning subsystems fabricated with easy-to-scale lithographic techniques and a distributed GPU software algorithm capable of meeting the processing and integration targets of the program based upon published vendor roadmaps and algorithms improvements.

The program demonstrated a working optical recirculating buffer capable of supporting a 12-line display system. The system demonstrated only 8.2dB loss per pass through the system. The team transferred the AO modulator design from BYU to MIT. MIT was able to fabricate the design using their direct write laser system. The direct write laser system is capable of printing on large format substrates. The team developed integrated signal outcoupling gratings that can also be fabricated using either direct laser writing or high speed lithography equipment.

The Phase I program identified commercially available advanced GPUs that provide a greater than 4-fold rendering engine performance increase and enable the system to generate data to meet the minimum performance requirements. The team has developed a roadmap that extends and optimizes the existing software to be capable of supporting a 1m × 1m full parallax holographic display suitable for command and control and intelligence applications. The analysis indicated that with additional software optimization and hardware improvements which are currently forecasted by industry roadmaps that the system is capable of generating data at rates exceeding 2TB/s.

6.0 RECOMMENDATIONS

The team will continue to address potential bottlenecks in the data generation and transmission pipeline including optimization of the recirculating optical buffer to reduce the data transfer requirements. The optical buffers would provide the leaky-module modulators with a persistence function so that they do not need to be refreshed at full bandwidth (~400kHz). This approach could reduce the problems that may arise as we begin to scale the display with more channels than we can directly drive with gen-locked GPUs. Creating image persistence to reduce the display drive bandwidth can simplify the drive electronics and improve the SWaPC performance of the overall system.

The team should continue to replicate and fabricate the modulator advances developed by BYU using the femtosecond laser. The MIT team should also perform an electrical comparison between the fs-laser fabricated devices and the devices produced by BYU to evaluate any performance differences.

The ultimate goal of this research effort is to develop a full-parallax, solid-state 3D display with no mechanically moving parts. The target system should be capable of achieving video-rate display speeds with electronically generated holograms, require no special viewing apparatus, and be able to use streaming video and streaming geometry together with existing static content.

To reach this goal, the team needs to achieve the following technical objectives: (a) optimize the performance of the display grating subsystems and validate the scalability and performance of the approach for Air Force's HVD application, (b) develop a "unit cell" display architecture based on display subunits that can be individually manufactured and assembled into a larger display. (c) demonstrate the performance of a one-unit system, and (d)demonstrate and validate a computer and display architecture capable of meeting the 15GB/sec transfer rate to achieve the threshold system requirements.

7.0 REFERENCES

1 Lloyd LaComb, Jr., Nasser Peyghambarian, Arkady Bablumyan, Rick Rankin, Armen Ordyan, Adina Morariu, V. Michael Bove Jr, Sunny Jolly, and Daniel Smalley, "Holographic Video Display Using Novel Guided-wave Scanning System (HVD-GWSS) Phase II," AFRL-RH-WP-TR-2016-0083, TIPD LLC, Tucson AZ, 59 pp (November 2016).
Distribution B. Available to qualified requesters at www.dtic.mil.

2 Lloyd LaComb, Jr., Nasser Peyghambarian, Arkady Bablumyan, Rick Rankin, Armen Ordyan, Pierre Blanche, V. Michael Bove Jr, Sunny Jolly, Daniel Smalley and Drew Henrie, "Holographic Video Display Using Novel Guided-wave Scanning System (HVD-GWSS) Phase II Extension," AFRL-RH-WP-TR-2018-XXX, TIPD LLC, Tucson AZ, 90 pp (January 2019).
Distribution B. Available to qualified requesters at www.dtic.mil.

3 Smalley, D.E., Smithwick, Q.Y.J., Bove, V.M., Barabas, J, Jolly, S., "Spatial light modulation via anisotropic leaky-mode coupling for holographic video displays", *Nature*, **498**, 20 Jun 2013, pp. 313-317.

4 N. Peyghambarian, L. LaComb, Jr., P-A. Blanche, A. Bablumyan, R. Rankin, A. Ordyan, P. St. Hilaire, R. Voorakaranam, C. Christenson, B Lynn, J. Wissinger, A. Chao, V. M. Bove, S. Jolly, M. Yamamoto, T. Gu, W. Hsieh, Y. Hu, I. Kitahara, W. Lin, B Rachwal, O. Siddiqui, S. Simavoryan, A. Sutin, J. Tillema, K. Ueno, and P. Wang, "3D Holographic Display Technology using Large Area Photorefractive Polymers (3DHDT-LAPP)," AFRL-RH-WP-TR-2011-0125, TIPD LLC, Tucson AZ, 126 pp (Nov 2011).
Distribution B. Available to qualified requesters at www.dtic.mil.

5 Martin, John, Holzbach, Mark, Riegler, Joseph, Tam, Chin, Smith, Adam, "Evaluation of Holographic Technology in Close Air Support Mission Planning and Execution", AFRL-RH-AZ-TR-2008-0025, Air Force Research Laboratory, 6030 South Kent Street, Mesa, AZ 85212

6 Stephen A. Benton and V. Michael Bove, Jr., Holographic Imaging, Wiley, Hoboken, NJ, USA, 2008

7 Kreis, T., Aswendt, P. & Hofling, R., "Hologram reconstruction using a digital micromirror device", Opt. Eng., 40, pp 926–933, 2001.

8 Hilaire, P., Benton, S., Lucente, M., "Synthetic aperture holography: a novel approach to three-dimensional displays", J. Opt. Soc. Am. A, 9, pp 1969–1977, 1992.

9 Lloyd LaComb, Jr., Nasser Peyghambarian, Arkady Bablumyan, Rick Rankin, Armen Ordyan, Adina Morariu, V. Michael Bove Jr, Sunny Jolly, and Daniel Smalley, "Holographic Video Display Using Novel Guided-wave Scanning System (HVD-GWSS)," AFRL-RH-WP-TR-2014-0035, TIPD LLC, Tucson AZ, 45 pp (Nov 2014).
Distribution B. Available to qualified requesters at www.dtic.mil.

10 https://www.nvidia.com/content/dam/en-zz/Solutions/design-visualization/technologies/turing-architecture/NVIDIA-Turing-Architecture-Whitepaper.pdf

11 https://image-us.samsung.com/SamsungUS/samsungbusiness/pdfs/DIGSIG-THEWALLPROFBRO-APR19T-Final-4-23-19.pdf

APPENDIX A - INTELLECTUAL PROPERTY, PUBLICATIONS AND PERSONNEL

A.1 Intellectual Property Resulting from This Program

A.1.1 Know How

A.1.2.1 TIPD, LLC. CUDA programming techniques, hogel generation algorithms and throughput optimization.

A.1.2.2 Massachusetts Institute of Technology. Femtosecond laser writing system development, grating writing using femtosecond lasers, acousto-optical modulator development and fabrication

A.1.2.3 Brigham Young University. Optical circular buffer design, fabrication, and testing, grating coupling techniques, optical multiplexing techniques, and acousto optical modulator design, development and testing techniques.

A.1.2 Trade Secrets

A.1.2.1 TIPD, LLC. Market requirements for commercial field-of-light-displays, CUDA programming optimization for hogel generation.

A.1.2.2 Massachusetts Institute of Technology. None to date

A.1.2.3 Brigham Young University. None to date

A.1.3 Trademarks

A.1.3.1 TIPD, LLC. None to date

A.1.3.2 Massachusetts Institute of Technology. None to date

A.1.3.3 Brigham Young University. None to date

A.1.4 Copyrights

A.1.4.1 TIPD, LLC. None to date

A.1.4.2 Massachusetts Institute of Technology. None to date

A.1.4.3 Brigham Young University. None to date

A.1.5 Patents

A.1.5.1 TIPD, LLC. None to date

A.1.4.2 Massachusetts Institute of Technology. None to date

A.1.4.3 Brigham Young University. Notice of allowance

Date Application Filed	USPTO Application Number	Title
4/17/2018	15/955646	Circular Buffers for Leaky Mode Displays

A.2 Publications and Presentations of Results from This Program

A.2.1 Joint Publications

None to date

A.2.2 TIPD, LLC

None to date.

A.2.3 Massachusetts Institute of Technology

Sundeep Jolly, Bianca Datta, Vik Parthiban, Daniel Smalley, and V. Michael Bove, Jr., "Experimental characterization of leaky-mode spatial light modulators fabricated by direct laser writing,"Proc. SPIE Practical Holography XXXIII: Displays, Materials, and Applications, 10944, 2019.

A.2.4 Brigham Young University

Pettingill, Daniel, Daniel Kurtz, and Daniel Smalley. "Static Structures in Leaky Mode Waveguides." Applied Sciences 9.2 (2019): 247.

A.3 Professional Personnel Associated with This Program

Company	Name	Role
TIPD, LLC	Professor Nasser Peyghambarian	Advisor
	Dr. Lloyd LaComb, Jr.	Principal Investigator Program Manager Software development and testing
	Dr. Arkady Bablumyan	Optical Design System Design Holography Theory
	Armen Ordyan	Optical Design HOE fabrication
	Richard Rankin (Rick)	System Design System Test
	Majid Behabadi	Purchasing
	James Fountain (Jim)	Finance
Massachusetts Institute of Technology (MIT)	Professor V. Michael Bove, Jr.	Co-Principal Investigator
	Sunny Jolly	Algorithm Development
	Bianca Datta	Femtosecond laser development and device fabrication
	Vik Parthiban	Femtosecond laser development and device fabrication
	Tyler Schoeppner	Femtosecond laser development and device fabrication
Brigham Young University (BYU)	Professor Daniel Smalley	Co-Principal Investigator AO and EO modulator development
	Dylan Barton	Circular Buffer Design and Fabrication

A.4 Advanced Degrees Awarded for Research Supported by This Program

A.4.1 Massachusetts Institute of Technology (MIT)

Sonny Jolly – Ph.D. awarded in February 2019

A.4.2 Brigham Young University (BYU)

None during this period

LIST OF SYMOBLS, ABBREVIATIONS, AND ACRONYMS

2D	Two dimensional
2.5D	Two and a half dimensional – a surface in 3D space
3D	Three dimensional
AFRL	Air Force Research Laboratory
ALMM	Anisotropic leaky-model modulator
AO	Acousto-Optical
AOC	Air Operations Center
AOM	Acousto-Optical Modulator
BOM	Bill of Materials
BYU	Brigham Young University
CAC	Command and Control
CAD	Computer Aided Design or Computer Aided Drawing
CGH	Computer generated hologram
COTS	Commercial-Off-the-Shelf (typically referring to commercially available products)
CPU	Central Processing Unit
CUDA	Compute Unified Device Architecture (NVIDIA development language)
CW	Continuous Wave (laser)
dB	Decibel
DLW	Direct Laser Writing
DP	Display Port (video display standard)
DPFLOPS	Dual precision floating point operations per second
DTED	Digital Terrain Elevation Data
DTIC	Defense Technical Information Center

DVI	Digital Visual Interface (video standard)
EO	Electro-Optical
EOM	Electro-Optical Modulator
FLOPS	Floating point operations per second
FOLD	Field of Light Display
FoM	Figure of Merit
FoV	Field of View
FoVi3D	FOLD system developer (Austin, TX)
FP	Full Parallax or Floating Point
GB	Gigabyte ($2^{30} \approx 10^9$ bytes)
GFLOPS	Gigaflops - 10^9 FLOPS
GHz	Gigahertz
GP	GigaPixels ($2^{30} \approx 10^9$ Pixels)
GPU	Graphics Processing Unit
HDMI	High-Definition Multimedia Interface (video standard)
HOE	Holographic Optical Element
Hogel	Holographic 3D Picture Element (**Ho**lo**g**raphic Pix**el**)
HPO	Horizontal Parallax Only
HVD	Holographic Video-Rate Display
HVD-GWSS	Holographic Video Display Using Novel Guidedwave Scanning System (predecessor program)
HWHM	Half-Width Half-Maximum
IARPA	Intelligence Advance Research Projects Activity
IR	Infrared
LC	Liquid Crystal

LCOS	Liquid Crystal on Silicon
LED	Light Emitting Diode
LIDAR	Light Detection and Ranging
LO	Local Oscillator
MB	Megabyte ($2^{20} \approx 10^6$ bytes)
MEMS	Micro-electrical Mechanical System
MHz	Megahertz
MIT	Massachusetts Institute of Technology
MP	MegaPixels ($2^{20} \approx 10^6$ Pixels)
N_B	Number of bytes per color channel (1 for this report).
N_C	Number of color channels in the HVD (1 for monochrome and 3 for RGB)
N_H	Number of display elements in the horizontal direction and $N_H \times N_V$ is the Number of Display Elements listed in Table 1.
N_V	Number of display elements in the vertical direction and $N_H \times N_V$ is the Number of Display Elements listed in Table 1.
N_Θ	Number of discrete views in the horizontal direction and Θ is the horizontal component of the conical FOV as specified in Table 1
N_Φ	Number of discrete views in the vertical direction and Φ is the vertical component of the conical FOV as specified in Table 1
NA	Numeric Aperture
NTSC	National Television System Committee (video standard)
NVIDIA	NVIDIA Corporation, Santa Clara, CA
OPSEC	Operational Security
OSG	OpenSceneGraph -open source 3D visualization software (www.openscenegraph.org)
PAL	Phase Alternating Line (video standard)
PE	Proton Exchange

Pixel	Picture Element
PL	Pulsed Laser
SAR	Synthetic Aperture Radar
SAW	Surface Acoustic Wave
SLM	Spatial Light Modulators
SMA	SubMiniature Version A – a type of coaxial connector
SMPTE	Society of Motion Picture and Television Engineers
SoA	State-of-the-Art
SPFLOPS	Single precision floating point operations per second
SWaP	Size, Weight and Power
SWEPPI	Space, Weight, Ergonomics, Power, Performance, and Integration
TB	Terabyte ($2^{40} \approx 10^{12}$ bytes)
TE	Transverse Electric
Tetrad	4-GPU computer used by TIPD for hogel generation
TFLOPS	Teraflops - 10^{12} FLOPS
TIPD	Tucson Integrated Photonics Design, LLC (Prime Contractor)
UV	Ultraviolet
VM	Visualization Manager
VMS	Visualization Manager System
Voxel	Volume element – a three dimensional extension of a pixel
Ω	Total number of bytes displayed on the HVD per second
Ω	Unit of resistance

GLOSSARY OF TERMINOLOGY

2D	**Two dimensional**. See also 2.5D and 3D. 2D data is a class of data that has a value at each point in a (typically) Cartesian grid. The values at each (x,y) position do not indicate the relationship between the points in the "z" direction. Examples include photographs where each point in the image has a particular intensity, TV images, and Google traffic maps.
2.5D	**Two and a half dimensional**. See also 2D and 3D. 2.5D data or displays provide some level of information about the z-relationship between the (x,y) points. Examples would include wire mesh models which when viewed in perspective provide some information about the z relationship between various (x,y) points. The data is displayed as one 2D image but with additional information that allows the viewer to determine more information about the scene. Other examples often considered 2.5D are contour maps and extrusion models in CAD software.
3D	**Three dimensional.** See also 2D and 2.5D. 3D data and displays provide the full (x,y,z) relationship between the data in the scene. 3D displays project at least two and up to 100s of different images to the viewer simultaneously. These images provide the viewer's visual system with a rich set of additional information allowing them to reconstruct the scene as if it were a "real" image. 3D displays are available in various formats that provide differing levels of visual clues. 3D glasses typically provide differing images to each eye whereas holographic display systems shape the phase of the light so that the eye focuses on the apparent emission point rather than the physical location of the emission to provide a more realistic 3D immersion.
AO	**Acousto-Optical or Acousto-Optics**. See also AOM, EO. Acousto-optical refers to the interactions between sound waves and light waves. The acoustic waves are generated by a transducer that converts electricity into mechanical motion. The mechanical motion is typically beyond the upper limit of human detection, often occurring at MHz or GHz frequencies. The sound waves generate changes in the refractive index of the medium through the photoelastic effect. These variations in the refractive index produced by the traveling sound waves cause the light to refract, diffract, or interfere.
AOM	**Acousto-Optical Modulator**. See also AO. An acousto-optic modulator uses a piezoelectric material (lithium niobate in this research) to generate travelling sound waves. These sound waves create a diffraction grating in the underlying medium that redirects the laser signal out of the medium towards the viewer to create an image. The spacing and strength of the sound waves can be controlled to change the angle of the light leaving the medium and provide different images at different angles. Complex acoustic waves can be created that redirect light from multiple locations along the length of the AOM to create an image with horizontal parallax.

EO	**Electro-Optical**. See also EOM, AO. The electro-optic effect refers to a change in the optical properties of a medium due to the presence of an electric field. In most cases the electrical field, typically in the MHz or GHz range, causes a change in the birefringence or refractive index of the optically transparent medium. The change in birefringence or refractive index redirects the path of the light.
EOM	**Electro-Optical Modulator**. See also EO, AOM. An electro-optic modulator uses the electro-optic effect to change the phase, frequency, amplitude, or polarization of an optical beam traveling through a medium. In this proposal, the phase of the individual beams are adjusted in a pattern that sweeps the beam along one axis to create parallax.
FP	**Full Parallax**. See also hogel, HPO. Parallax is the visual displacement of the position of an object when viewed from two different locations. Full parallax refers to a display system that provides parallax clues as the viewer moves along both the horizontal and vertical directions. In full parallax displays, each emitter in the display generates a pyramid of light with each ray in the pyramid carrying unique information.
Hogel	**Holographic 3D Picture Element** (**Ho**lo**g**raphic Pix**el**). A point on the physical display that emits a pyramid of light. In the HVD display, the number of hogels is determined by the acoustic pattern generated by the AOM rather than being a fixed number determined by the fabrication process. The number of hogels per AOM is limited by the bandwidth of the AOM. For an HVD HPO system, the number of hogels is related to the bandwidth through the equation $Bandwidth \geq Number\ hogels * Number\ views/hogel$.
HPO	**Horizontal Parallax Only**. See also FP, hogel. Parallax is the visual displacement of the position of an object when viewed from two different locations. Horizontal parallax only refers to a display system that provides parallax clues in only the horizontal direction. Horizontal parallax is critical for a 3D display so each eye receives the correct viewpoint and the brain can create a three dimensional scene. In horizontal parallax only displays, each emitter in the display generates a pyramid of light but while each ray emitted along a horizontal line carries unique information, the information in the vertical axis is a copy of the corresponding information on the horizontal axis.
SAW	**Surface Acoustic Wave** also refers to a device that generates surface acoustic waves. See also AOM. A surface acoustic wave is a traveling acoustic wave that propagates primarily in one direction along the surface of a material. In this proposal, the AOM generates surface acoustic waves that create a diffraction grating and diffract the laser beam to create the image.
SLM	**Spatial Light Modulators**. A spatial light modulator is a two dimensional device that alters some property of the light beam. The SLM can work in either transmission or reflection and alter the phase and/or amplitude of the light beam.

SLMs can be controlled at the level of an individual pixel. SLMs are used to shape the wavefront of the beam into the desired form. SLMs can be made from liquid crystals, liquid crystal on silicon (LCoS), MEMS, or other exotic materials. Their most common use is in TVs and overhead projectors.

SWEPPI **Space, Weight, Ergonomics, Power, Performance and Integration**. An acronym defining a number of the key parameters needed for successful introduction into integration into an existing workflow.

TE/TM **Transverse Electric and Transverse Magnetic.** Light travelling a waveguide, through a fiber, or emitted by a laser will have one or more spatial modes in additional to its frequency. The spatial modes arise when the light is confined to a spatial region. The boundary conditions of the region limit the solutions to Maxwell's equations to standing waves that are integer multiples of the fundamental mode (lowest spatial frequency). TE and TM refer to the two orthogonal directions relative to the direction of propagation.